EPA

Radiation

A Study of Radioactive Airborne Effluents From Particle Accelerators
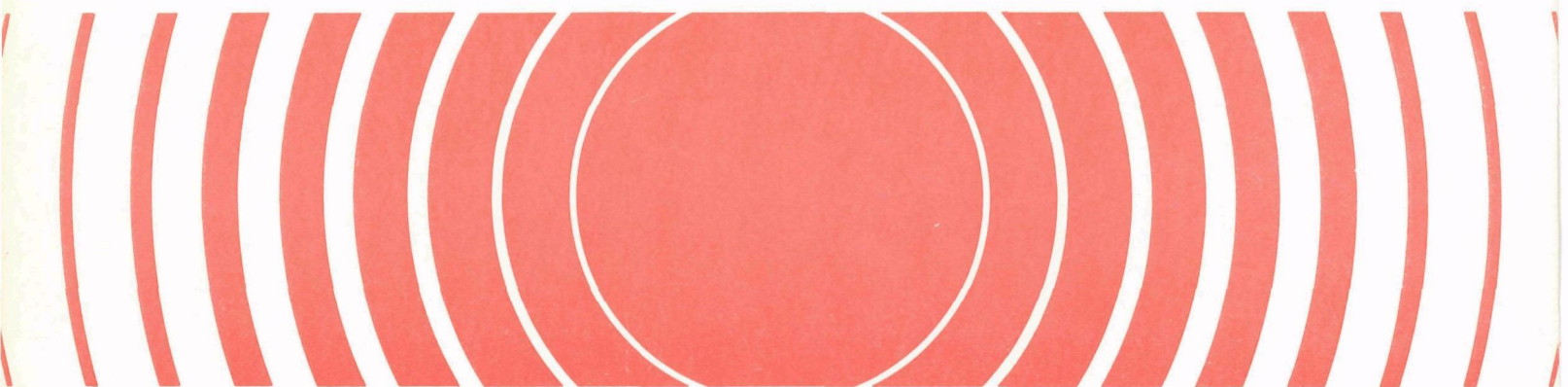
ERRATUM

This technical note, <u>A Study of Radioactive Airborne Effluents From Particle Accelerators</u>, was printed with the wrong sequential number. The number on the cover and title page should read ORP/TAD-79-12. Please make the appropriate changes with pen and ink.

A STUDY OF RADIOACTIVE AIRBORNE EFFLUENTS
FROM PARTICLE ACCELERATORS

Final Contract Report
Principal Investigator: Joel I. Cehn
Teknekron Research, Inc.
1486 Chain Bridge Road
McLean, Virginia 22101

August 1979

Prepared for
U.S. Environmental Protection Agency
Under Contract No. 68-01-4997

Project Officer
Frederick C. Sturz
Office of Radiation Programs (ANR-459)
U.S. Environmental Protection Agency
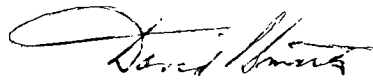Washington, D.C. 20460

DISCLAIMER

This report has been reviewed by The Office of
Radiation Programs, U.S. Environmental Protection
Agency (EPA) and approved for publication. Approval
does not signify that the contents necessarily
reflect the views and policies of the Environmental
Protection Agency, nor does mention of trade names
or commercial products constitute endorsement or
recommendation for use.

Secion 122 of the Clean Air Act Amendments of 1977, Public Law 95-95,
directed the Administrator of the Environmental Protection Agency, to review
all relevant information and determine whether emissions of radioactive
pollutants into the ambient air will cause or contribute to air pollution which
may reasonably be anticipated to endanger public health. As part of this
review, the Agency has been assessing the public health impact resulting from
emissions of radioactive material into the air from a broad spectrum of source
categories. This study was performed to assess the extent of radioactive
airborne emissions from non-government owned particle accelerators.

Readers of this report are encouraged to inform the Office of Radiation
Programs of any omissions or errors. Comments or requests for further
information are also invited.

David S. Smith
Director
Technology Assessment Division (ANR-459)
Office of Radiation Programs

ABSTRACT

This report discusses radioactive gas production around non-Federally owned particle accelerators, and the release of such gases to the atmosphere. The estimated 1200 non-Federally owned accelerators in the United States are categorized by type and energy, and the potential for radiogas production is discussed for various types. The results of field monitoring around two machines (a cyclotron and a Van de Graaff) are also presented. Estimates of annual radiogas releases from generic accelerator facilities are made. The isotopes of interest are: tritium (target gas) from a generic Van de Graaff; nitrogen-13, oxygen-15 and carbon-11 from a generic cyclotron; and argon-41 from a generic linac. Finally, control technologies to reduce airborne releases of these isotopes are discussed.

TABLE OF CONTENTS

TABLE OF CONTENTS (Continued)

LIST OF FIGURES

LIST OF TABLES

1.0 INTRODUCTION

On August 7, 1977, the President signed into law the Clean Air Act Amendments of 1977. These amendments extended the definition of "air pollutant" to include radioactive material that is emitted into the ambient air. Also, Congress directed the Administrator of the Environmental Protection Agency (EPA) to investigate the emissions of radioactive pollutants with respect to public health. This study is an investigation of the effluents from selected particle accelerator facilities.

The sources of these potential radioactive effluents are discussed in Sections 4.0 and 5.0. Section 5.0 also contains the results of effluent monitoring performed at two study facilities. A discussion of air treatment systems capable of reducing these effluents is contained in Section 6.0.

Also presented in this report is an overview of the use and distribution of accelerators in the United States (Section 3.0) and a discussion of the various types of accelerators and how they work (Section 2.0). Finally, a summary of our findings and our conclusions is presented in Sections 7.0 and 8.0.

It should be noted at this point that this study is restricted to non-Federally owned accelerators. Airborne effluents from the large and very large machines at the national laboratories (e.g., Brookhaven) and elsewhere (e.g., National Bureau of Standards) are the subject of a concurrent study. Thus, we have focused on machines at universities and in the private sector, which generally range in energy up to about 100 MeV.

Finally, this study focuses on machines not used exclusively for the production of radiopharmaceuticals. Discussions of airborne effluents from these sources are included in a separate report, "A Study of Airborne Radioactive Effluents from the Radiopharmaceutical Industry," recently completed by Teknekron for EPA/EERF.

2.0 PRINCIPLES OF ACCELERATOR OPERATION

2.1 General Design Considerations

Generically, accelerators are devices for imparting high kinetic energies to electrons or to positively charged particles (such as alpha particles, protons, and deuterons) by electric or magnetic fields. In typical operation, the stream of accelerated particles, which travel in an evacuated tube or other enclosure within the machine, impinges on a metallic or gaseous target, producing various types of secondary radiation. Those types with the highest associated energies, neutrons and X-rays, are of principal importance in terms of practical application, such as industrial radiography, X-ray therapy, and radioisotope production. In some designs the target is enclosed within the accelerating tube, while in others it is external to the vacuum. In the latter case, the particle beam leaves the tube via a foil window so that it travels through air for an appreciable distance before reaching the target. In certain applications, such as electron beam tumor therapy, the primary particle beam is used directly, rather than as a means for generating secondary radiation.

In terms of basic design, accelerators are often categorized according to the means used to achieve the desired particle velocity. For the most part, they fall into the following three main classes:

- Constant D.C. Field Machines

    Accelerators in this class, sometimes called "potential-drop" machines, share the common feature of a constant D.C. electric field through which the charged particles "fall." Depending on the polarity of the accelerating field with respect to the particle source, machines of this type can be used for accelerating either negatively or positively charged particles. Within this class, the most important accelerator designs are the Cockcroft-Walton and Van de Graaff machines which are named after the developers of the original prototypes. The Dynamitron and the insulated core transformer (ICT) accelerator are constant D.C. field machines based on the Cockroft-Walton design.

● Incremental Acceleration Machines

In these machines, the particles are incrementally accelerated by time varying electric fields, so that their velocity increases in a stepwise rather than continuous manner. The most common types in general use are the linear accelerator (linac) and the cyclotron and its derivative designs.

● Magnetic Field Accelerator

The only current example of this category is the betatron in which electrons are accelerated by a time varying electric field which, in turn, is derived from a time varying magnetic field. Acceleration is not incremental.

Some machines do not fit exactly into any of the above three categories. For example, neutron generators are so classified in terms of function, rather than by the accelerating principle employed. In these devices, neutrons are typically produced by the impingement of accelerated deuterons on a tritium target. Some designs employ Cockcroft-Walton type high voltage power supplies for generating the accelerating field, so that these are constant D.C. field machines. Others, however, are self-rectifying, so that the electric field actually consists of a series of half-wave pulses having a repetition rate equal to the frequency of the source A.C. voltage. Such a field is equivalent to a D.C. field with a superimposed "ripple" component. It is not a constant D.C. field. Another accelerator type that is not categorizable under the above classification is the resonant transformer machine. In this design, the high voltage is produced by resonating the transformer inductance with the distributed capacity of the system. The frequency of the current supplied to the primary winding is usually higher than ordinary line frequency (60 Hz) because the system capacity is relatively low. Resonant transformer machines typically operate in the self-rectifying mode, so that the accelerating field generated is not one of constant D.C. potential.

Before a discussion of the machines themselves, it is important to consider the topic of relativistic mass increase because this factor strongly influences the design of several accelerator types. As predicted by Einstein, the mass of a moving body has been found not to be independent of its velocity when measured with respect to a given reference framework. The quantitative relationship between the mass of a body moving at a velocity (v) and the mass

of the body at rest is shown by the following expression in which b = v/c (c is the velocity of light = 300,000 kilometers/second), m is the moving mass, and m_0 the rest mass:

$$m/m_0 = \sqrt{\frac{1}{1 - b^2}}$$

As is evident, when the velocity is very small compared with that of light, the term b is essentially zero so that m is virtually equal to m_0. However, at velocities that are comparable with that of light, b is no longer negligible, with the result that the m/m_0 ratio can become quite large. For example, for b = 0.9, m/m_0 is about 2.3; for b = 0.999999999, m/m_0 is approximately 22,360. In the limiting case, m approaches infinity as v approaches c.*

At relatively low energy levels, the relativistic increase in mass is small for accelerated positive particles but may be quite appreciable for electrons. The kinetic energy of a particle (K), in terms of its mass and velocity, is given by $K = mv^2/2$. Inasmuch as the rest mass of an electron is only about 1/1830 that of a proton, for any value of K an electron must be accelerated to a considerably higher velocity than a proton. For example, at K = 11 MeV** an electron must have been accelerated to a velocity of about 0.999 that of light. At this velocity, its m/m_0 ratio would approximate 22. On the other hand, a proton accelerated to the same energy level would be moving at a velocity of only a little more than 0.1 light speed and its m/m_0 ratio would be less than 1.005.

2.2 Principal Accelerator Design Features

This section describes the major design features of the different accelerator classes identified in Section 2.1.

---

*Note that if a body were to be accelerated to a velocity approaching c, the required force (force = mass x acceleration) would approach infinity as the mass approached infinity. As the expression shows, if the force failed to approach infinity, the acceleration produced by it would progressively fall as the mass increased, reaching zero in the limiting case. The speed of light is, therefore, an unattainable velocity limit for anything possessing mass.

**This expression means 11 million electron volts. The incremental kinetic energy gained by an electron as a result of its acceleration by a one-volt electric field is defined as one electron volt. The electron volt is a common unit of measure in the context of particle acceleration.

2.2.1 Constant Field Machines

Cockcroft-Walton Accelerator

This design was employed in the first accelerator constructed (1932) and is still employed for particle acceleration to energy levels up to about 1 MeV. The high voltage D.C. accelerating field is produced by rectification of the output of a high potential power transformer in a voltage doubling circuit. The net result is the development of a D.C. potential that is theoretically* twice the peak of the A.C. voltage appearing across the transformer secondary winding. The principle of operation is shown in Figure 2-1. When the high voltage appearing at terminal A of the secondary winding passes through the positive half of the A.C. cycle, rectifier R_1 conducts, thus charging capacitor C_1 to a positive D.C. potential equal to the peak voltage of the half sine wave, as shown in the figure. During the second half of the cycle, the sign of the potential at A is negative and R_1 does not conduct. However, R_2 now conducts so that the capacitor C_2 charges to the peak negative value of the applied voltage. Since C_1 and C_2 are connected in series, the total voltage appearing across the two is twice the peak voltage.

The effectiveness of this system in maintaining a constant D.C. accelerating voltage largely depends on the relationship between the magnitudes of the charging and load (due to the particle beam) currents and on the capacitor sizes. If the load current is small in comparison with the charging current, the potential across the capacitors will decline only slightly between successive peaks in the A.C. cycle. As the load current increases, the D.C. potential will drop progressively between these peaks so that its <u>average</u> value could fall significantly below twice the peak value. This effect is called "regulation." It is significant because a change in the field potential will directly affect the kinetic energies of the accelerated particles

---

*The D.C. potential would be exactly twice the peak voltage if the electrical components were ideal and if there were no current drain from the circuit, either from extraneous losses or the particle beam.
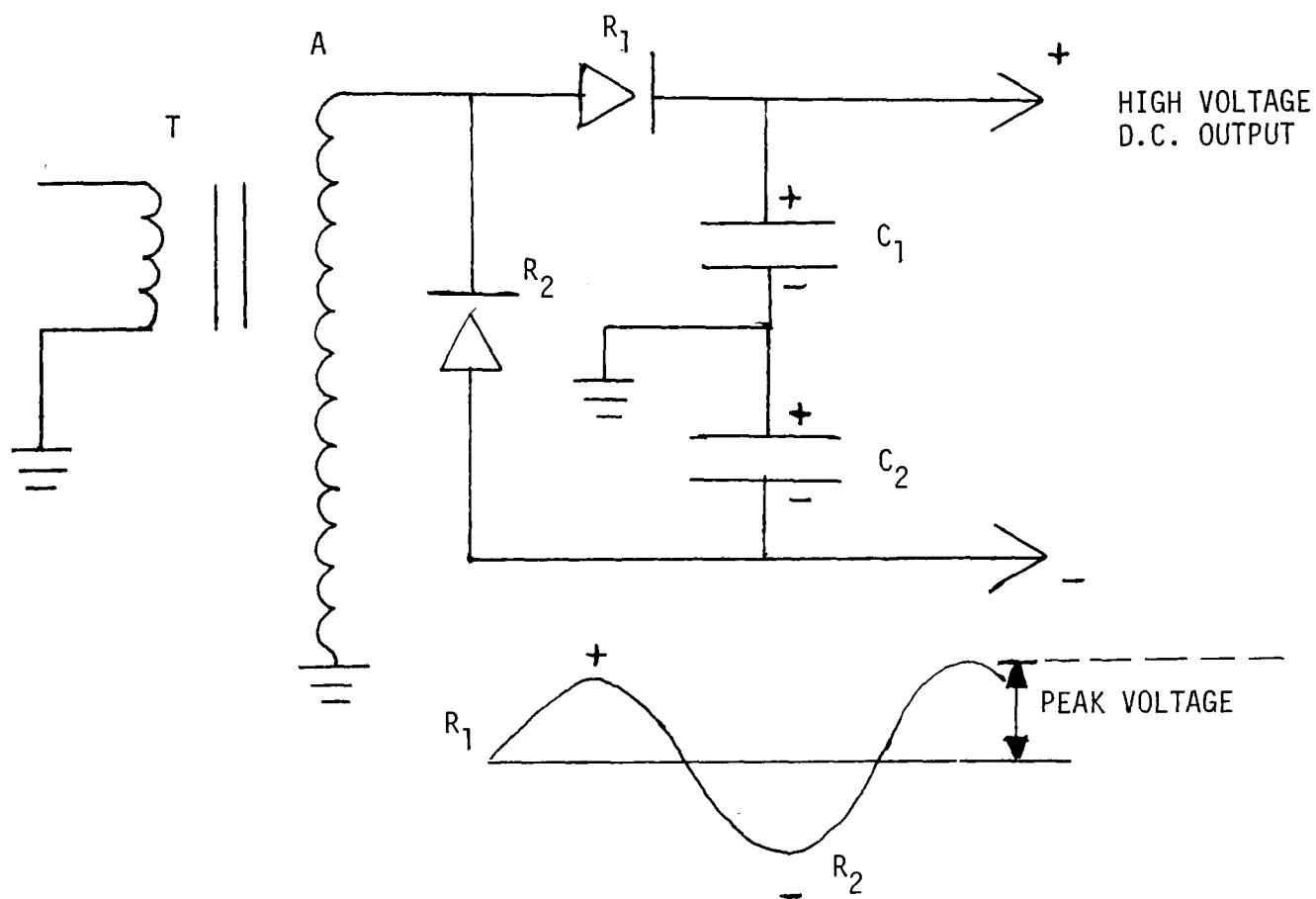
FIGURE 2-1

OPERATING PRINCIPLE OF A VOLTAGE DOUBLER

which must usually be accurately maintained at known values in experimental studies. Typically, these accelerators are equipped with voltage control devices that permit precise setting of the D.C. field potential under the load imposed by the beam current which may range from microamperes to several milliamperes.

Van de Graaff Generator

This machine employs a moving belt of insulating material which operates as an electric charge transfer device. High potentials are generated by charge accumulation. As Figure 2-2 shows, the charge is produced by a high voltage power supply and transferred to the belt via electrode A. As the belt moves in the direction shown by the arrows, the charge is transferred by electrostatic induction to the metal shell C via electrode B. This device is based on the principle that the potential (V) at a point, produced by a charge (q), at a given distance from the point (r), in a medium of dielectric constant (n) is given by the relationship:

$$V = \frac{q}{nr}$$

Inasmuch as n is a constant (unity in a vacuum, and very close to unity in most gases) and r is determined by the machine design, the voltage developed depends solely on how much charge can be transferred to C and maintained. A major limiting factor is the breakdown potential of the air surrounding the charged sphere. This potential can be substantially increased by operating the machine in either a vacuum or a high-pressure ambient atmosphere. The latter procedure is generally employed. It is usual practice to house the machine within an enclosure that is pressurized (with either air or some other gas) to about 10 atmospheres. Under these conditions, potentials of the order of 10-12 megavolts can be maintained. Small machines designed to generate relatively low potential accelerating fields (less than one megavolt) do not require pressurization.

ION OR ELECTRON SOURCE

HIGH VOLTAGE TERMINAL

C

B

CORONA POINT
VOLTAGE CONTROL

INSULATING COLUMN &
EQUIPOTENTIAL RINGS

PRESSURE TANK

ACCELERATING COLUMN

HIGH VOLTAGE
POWER SUPPLY

A

BELT DRIVE

VACUUM PUMP

PRESSURIZING
GAS SUPPLY

BEAM
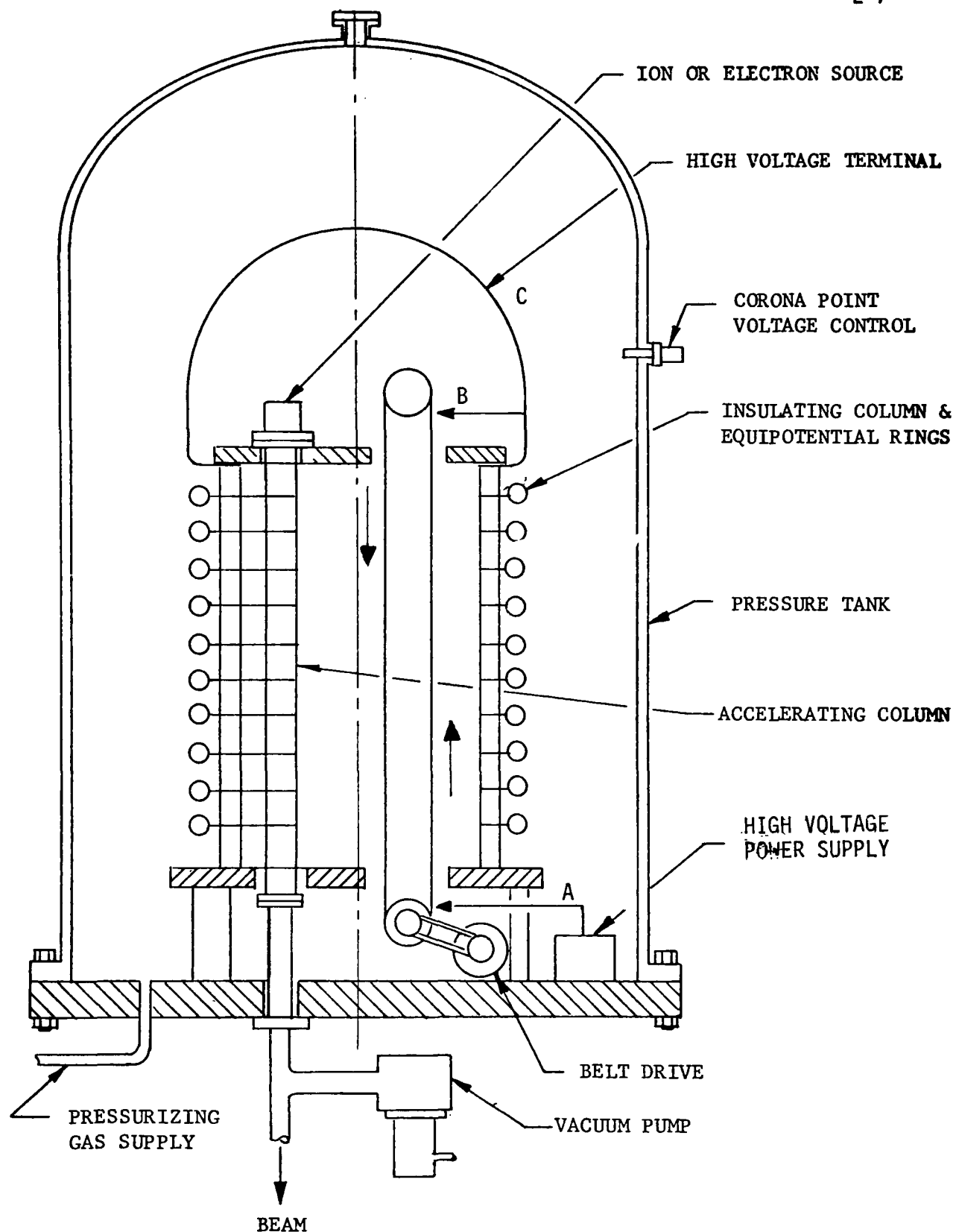
FIGURE 2-2

DESIGN OF A VAN DE GRAAFF GENERATOR

Higher particle energies can be attained through "tandem" arrangements of these machines. For example, in the two-stage tandem Van de Graaff generator, negative ions are accelerated in the first stage toward the positive terminal located at the center of the machine. This terminal houses a gas-filled channel through which the ions travel. During this exposure, they lose their negative charges and are converted to a positive ion beam. In the second stage, this beam is further accelerated toward the ground potential terminal at its end. Three-stage Van de Graaff accelerators have also been constructed.

All constant field machines have the disadvantage of requiring high voltage D.C. sources with the attendant problems of insulator leakage and corona loss due to ionization of the surrounding air. These problems become more severe with increasing voltage and limit the maximum potentials that are practicably attainable and, hence, limit the maximum kinetic energies that can be imparted to the accelerated particles. In the next class of machines to be discussed, these difficulties are eliminated by successively applying relatively weak accelerating fields whose cumulative effects permit the attainment of far higher energy levels than can be achieved with constant field machines.

2.2.2 Incremental Acceleration Machines

Linear Accelerator (Linac)

The basic design of this machine is illustrated in Figure 2-3. In essence, this accelerator consists of a series of coaxially arranged metal tubes, with gaps between them, alternately connected to the same terminal of a high frequency sine wave generator. The tube assembly is enclosed within a vacuum. Electrons are injected at point A and travel in the direction shown by the arrow. In the drawing, an electron is shown as about to enter the gap between tube 1 and tube 2. Assume that the time of entry coincides with the time at which the phase of the applied voltage is such that tube 2 is positive with respect to tube 1. The electron will thus accelerate during its passage
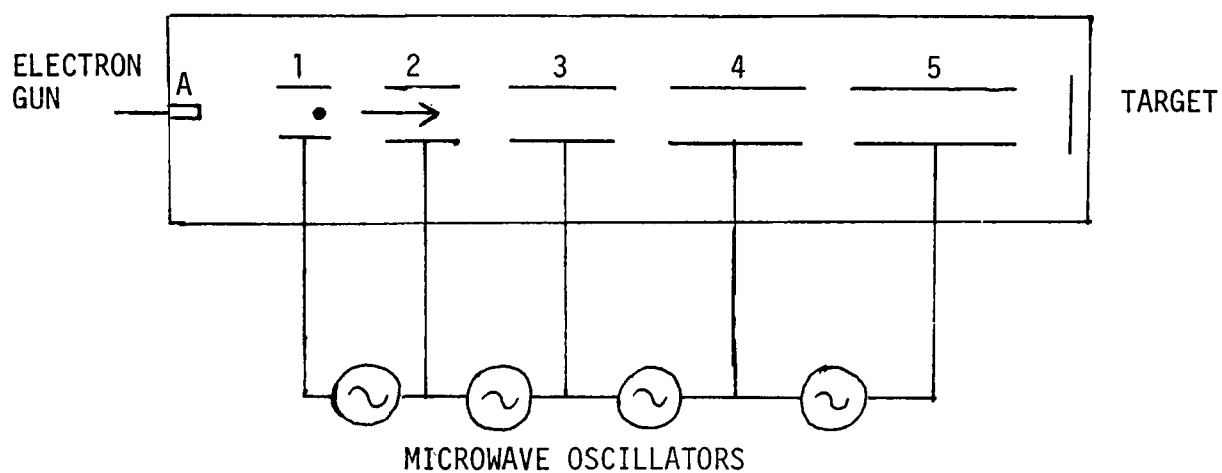
FIGURE 2-3
BASIC DESIGN OF A LINEAR ACCELERATOR

across the gap. By the time it has reached the beginning of the next gap (between tubes 2 and 3), the driving voltage has passed through a complete cycle so that tube 3 is electrically positive with respect to tube 2, thus further accelerating the electron. (Since there are no potential gradients <u>within</u> the tubes, the electrons experience acceleration only when moving through the gaps between them.) It will be noted from Figure 2-3 that the tube lengths increase progressively in the direction of electron beam travel. This increase in <u>length</u> compensates for the decrease in the <u>time</u> required for an electron to travel a given distance along its total path as its velocity increases. If the tube lengths are appropriately selected with respect to the frequency of the driving potential and the increasing particle velocities, with consequent relativistic mass effects taken into account, the electrons will arrive at each gap at a time when the tube it is approaching is positive with respect to the tube it is leaving.

The above discussion presents the linac as an electron accelerator because all the early machines were designed for this purpose. At present, however, proton linear accelerators are also made. Their basic principle of operation is the same, except that proton entry into an inter-tube gap occurs when the tube ahead is negative with respect to the one behind. A major application of electron linacs is radio- and electron-therapy. These machines are often designed so that either X-rays (resulting from the impingement of the electron beam on a target) or the primary electron beam itself can be employed. Proton linacs are used primarily for research purposes.

Cyclotron

Like the linac, the cyclotron uses an alternating electric field for incrementally accelerating the particle beam. However, as the name of the machine implies, the beam path is circular, rather than straight. Figure 2-4, an illustration of the features of the cyclotron, shows that the key components of the cyclotron include two semicircular hollow shells (called "dees" because of their shape). The dees, which are made of metal, are enclosed within a

Deflector Plate   Outlet   Target Chamber   Dee   A   O   S   B   Dee   Metal Tank
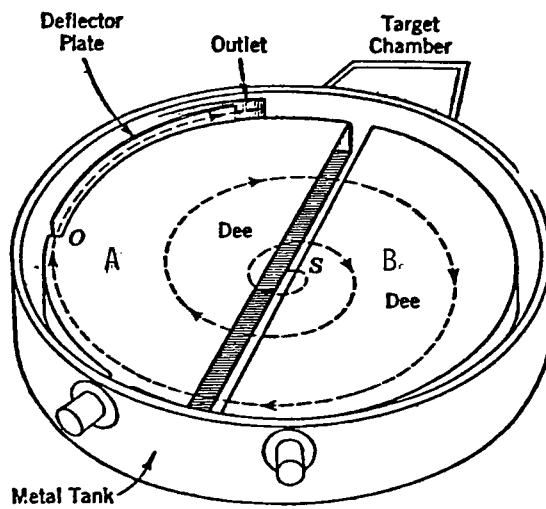
FIGURE 2-4

PRINCIPLES OF A CYCLOTRON

metal tank which is evacuated and connected to an alternating current generator that supplies the accelerating voltage. Not shown in the figure is a magnet structure whose pole pieces are parallel with the upper and lower dee surfaces and which exerts a centrally directed uniform radial magnetic field. The gap between the two dees is functionally analogous to those between the tubes in the linac. The particles are accelerated only when moving across the gap because there is no potential gradient within the dees. The basic operating principle is as follows: a positive ion introduced from the source S at a time when dee B is negative with respect to dee A would be accelerated toward dee B and, in the absence of the imposed magnetic field, would move within it in a straight line at constant velocity. Because of the magnetic field, however, the ion will be constrained to a path of constant radius while it remains within dee B. The radius is constant because while the particle is within a dee, its velocity is not exposed to tangential accelerating forces and remains unchanged. During this time, the centripetal and centrifugal forces on it are equal. The centrifugal force is expressed by Mv^2/r, where M is the particle mass and r the radius of its path. The centripetal force is given by Hev, where H is the magnetic field intensity and e is the charge associated with the particle. Thus,

$$Hev = \frac{Mv^2}{r}, \text{ so that } r = Mv/He$$

Therefore, for a constant velocity, r is constant because M, V, H, and e are also constant. (It is assumed for the moment that relativistic effects can be ignored, permitting M to be treated as constant. These effects will be considered later.) Hence, the path described by a particle traveling within a dee is a semicircle (ignoring the half-width of the gap). When the particle leaves dee B and enters the gap in its approach to dee A, it is exposed to the accelerating field between the dees, and thus its velocity increases. Since r = Mv/He, r must increase. Thus, on entering dee A, the ion describes a semicircular path of slightly greater radius than that followed previously in dee B. From the foregoing, it is clear that most of the total ion path within

the cyclotron consists of a series of semicircles of progressively larger radii. When the ion reaches the periphery of dee A, it is deflected outward by a negatively charged electrode into the target chamber.

In order to accelerate the particles with a time varying electric field of constant frequency, it is necessary that they always arrive at a gap when the potential gradient across the dees is of the correct polarity regardless of their path radii at the arrival time. Expressed somewhat differently, their angular velocity (w) must be constant and, therefore, independent of their linear velocity (v). That this condition is met (assuming particle mass to be constant) is easily demonstrated. The angular velocity (w) is equal to v/r. Thus, r = v/w. If v/w is now substituted for r in the equation r = Mv/He, we find that

$$w = He/M$$

For any given positive particle (proton, alpha particle, deuteron, etc.), the e/M ratio is characteristic of the particle type. Therefore, the angular velocity and thus the traverse time per semicircle is determined only by the magnetic field intensity. once the category of particle to be accelerated has been chosen. Note that v does not appear in the equation, so that w is independent of v and, hence, of r. In practice, it is usual to maintain the field at a fixed intensity (regardless of particle type) and to adjust the frequency of the accelerating field so that it will be in synchronism with w, as determined by both the e/M ratio of the particle type to be accelerated and the magnetic field intensity setting. At typical magnetic field intensities, the accelerating electric field frequencies are of the order of several megacycles per second (MHz). For example, if a machine's magnetic field intensity has been set to 15,000 gauss, the accelerating frequency for protons would be approximately 23 MHz. In the case of deuterons (He^{2+} ions), the e/M ratio is one-half that of protons, so that the accelerating frequency for these ions (assuming the same value of H) would be 1/2 x 23 MHz.

An important characteristic of a cyclotron is the maximum final energy attainable for a given particle accelerated within it which, as will be shown, is

directly related to the machine dimensions. This energy can be readily
derived by squaring the expression for the path radius shown above, giving

$$r^2 = \frac{M^2 v^2}{H^2 e^2}$$

Kinetic energy $= K = 1/2\ Mv^2 = \frac{H^2 e^2}{2M} r^2$

As the last expression indicates, the kinetic energy of a particle of a given
type constrained to a circular path by a given value of H is directly propor-
tional to the square of the radius of that path. If r is taken to be the
radius of the final semicircle traversed by the particle before ejection from
the dee, the final attainable energy is thus essentially determined by the
radii of the dees. This is why high energy cyclotrons must be larger than
lower energy machines.

The final energy attained by a particle is independent of the incremental
kinetic energy acquired during each of its passages across the gaps between
the dees. Nevertheless, it is obvious that the final energy must be the
aggregate of these increments. It follows that the total number of revolutions
made by a particle within the cyclotron to attain a given energy level will be
fewer for stronger than for weaker electric accelerating fields. Ordinarily,
the number of complete orbits made by a particle is on the order of hundreds
of thousands.

In the discussions of the cyclotron to this point, any effects due to rela-
tivistic increases of particle mass have been deliberately ignored (i.e.,
the mass was assumed to remain constant) so that the angular velocity (w)
could then be considered as constant for a given magnetic field intensity
and particle type. Because of the constancy of w, the applied accelerating
A.C. voltage could be maintained at an invariant frequency and the arrival
of a particle at a gap would always occur when the potential across the gap
was appropriately phased. Cyclotrons of this type are sometimes called "fixed
frequency machines." The assumption of constant particle mass is essentially

valid for positive particles, provided that they are accelerated in relatively low energy cyclotrons. For example, if a proton were accelerated to an energy level of about 4.7 MeV, the ratio of moving mass to rest mass (m/m_o) would be only 1.005 (the corresponding velocity would be approximately one-tenth that of light). The constant mass assumption does not, however, apply to electrons. As previously explained, because of their relatively low rest masses (approximately 1/1830 of a proton mass) they must be accelerated to quite high velocities to attain even moderate energy levels. At 4.7 MeV, an electron would have an m/m_o ratio of over 10 and a velocity of more than 0.995 that of light. Because of the large increase of electron mass at even comparatively low energy levels, it is evident that their angular velocities would not remain constant if accelerated in a cyclotron, but would decline substantially so that phase synchronization with a fixed frequency accelerating field would soon be lost. For this reason, cyclotrons are not suitable as electron accelerators.

Relativistic increases in proton mass cannot be ignored when these particles are accelerated to higher energy levels. However, these increases are far less extreme than the increases in electron mass. For example, the proton m/m_o ratio at 625 MeV is somewhat less than 1.7; at 1200 MeV it is about 2.29. The magnitudes of these ratios are low enough so that they can be accommodated by appropriate modifications of the basic cyclotron design without loss of phase synchronization.

In some machines, the relativistic mass effect is compensated for by a nonuniform magnetic field which is stronger at the periphery of the dee than at its center. It will be recalled that the angular velocity (w) of the accelerated particles is equal to He/M. From this relationship, it can be seen that if the magnetic field is shaped so that its intensity increases radially at the rate of the relativistic increase in proton mass, the ratio H/M will be constant and, consequently, w will also remain constant. Machines designed in this manner can accelerate protons to higher energy levels with fixed frequency A.C. generators than can those machines with radially uniform magnetic fields. They suffer, however, from the fact that radial field shaping tends to defocus the particle

beam. This defocusing effect can be largely overcome by special contouring of the faces of the magnet pole pieces. Accelerators incorporating this feature are sometimes called "sector focused" or "azimuthally varying field" (AVF) cyclotrons. These machines permit the attainment of energy levels of the order of hundreds of MeV.

Frequency modulation is a quite different approach to compensating for relativistic mass increase. As pointed out, the effect of this mass increase, given a uniformly radial magnetic field, is to reduce the angular velocity of the particles. This limits the final energy that can be attained in a fixed frequency machine because of progressive loss of synchronization between the particle arrivals at the gaps between the dees and the accelerating A.C. voltage. It is evident that higher energy levels could be attained if the accelerating voltage frequency were gradually reduced as the particles spiraled outward so that it always stayed "in step" with the decreasing angular velocity of the particles. This technique has been implemented, and machines based on this principle are called "synchrocyclotrons."

It was originally believed that achieving synchronization between the accelerating field frequency (f) and the decreasing angular velocity (w) of the particles might prove difficult. However, the "principle of phase stability," discovered in 1944-45, indicates that sychronism will occur more or less automatically. Suppose that the machine is designed so that the particles enter the gap during the 90°-180° portion of the sinusoidal accelerating waveform. Now assume that there is a slight mismatch between f and w such that a particle, in crossing a gap, receives slightly more energy than it should. In this case, its relativistic mass increase will be slightly higher than it would normally be, and its semicircular path through the dee will require correspondingly more time. Therefore, it will be late in its arrival at the next gap with respect to the accelerating voltage wave which will have passed its 90° peak. In consequence, the particle now will receive somewhat less energy than it would have if synchronization had been precise. Conversely, a particle that originally received too little energy during a gap crossing will experience a smaller relativistic mass increase and it's angular velocity will be correspondingly

higher. Therefore, it will arrive at the next gap somewhat earlier during the 90°-180° portion of the accelerating voltage wave and will thus receive more energy during its transit through the gap. This self-correcting mechanism does not attain phase stability in the absolute sense of a rigid relationship in time between particle arrival at a gap and the appearance of a particular point of the accelerating voltage waveform. Actually, the orbit periods tend to oscillate about a mean value from which they vary by quite small amounts. These oscillations are known as "synchrotron oscillations," and their frequencies are usually considerably less than the revolution frequency (1/w).

As is evident from the foregoing, particle acceleration occurs during only a fraction of the total sinewave cycle. In a synchrocyclotron, stable orbits are formed by particles reaching the first transit during approximately 1% of the cycle, so that the beam is actually discontinuous. It consists of a series of bursts of pulses. Because of this low duty cycle (i.e., ratio of beam pulse duration to the total period of one sinusoidal cycle), the average beam currents generated in these machines tend to be lower than those produced in constant frequency machines in which the effective duty cycles are longer.

2.2.3 Magnetic Field Accelerator (Betatron)

First developed in 1940, the betatron was initially conceptualized as an approach to imparting higher energies to electrons than had been attained by other means. Betatrons can produce electron beams with energies on the order of several tens of MeV (one machine in operation at the University of Illinois is rated at about 300 MeV). In the past, the therapeutic use of betatrons in hospitals was not uncommon, but they have been displaced by linacs for this application to a considerable extent.

The principal betatron design features are shown in Figure 2-5. Basically, this machine consists of an alternating current magnet within whose field is located a circular evacuated tube ("doughnut") within which the electrons
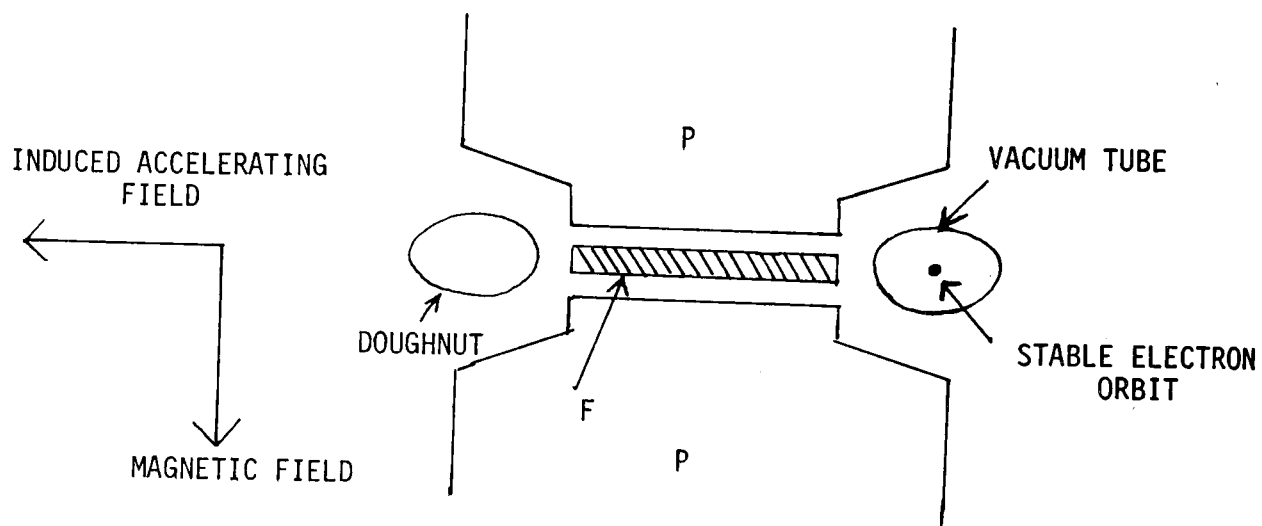
FIGURE 2-5
CUTAWAY VIEW OF A BETATRON

are accelerated. The electrons are usually injected into the doughnut
in pulses from an electron gun (i.e., an electron source and associated
D.C. accelerating electrodes) with initial energies of a few tens of keV.
Between the pole pieces of the magnet, identified as P in the illustrations,
is a "flux bar" (F). By inserting flux bars with different magnetic satura-
tion characteristics, the maximum energy attained by the electrons can be
controlled.

The betatron operates according to the following principles. The sinusoidally
alternating magnetic flux, whose frequency is typically a few hundred Hz
(cycles per second), induces an A.C. emf (electromotive force) of the same
frequency that is exerted tangentially with respect to the electron orbit
within the tube. The magnitude of the accelerating emf is maximum when the
time rate of change of the magnetic flux is maximum. The latter condition
occurs when the sinusoidal flux is passing through its zero value. The
pulse repetition rate of the injected electron burst is synchronized with
the frequency of the magnetic field and is so phased that the electrons enter
the doughnut about when the field is changing sign (i.e., passing through zero).
Thus, the rate of particle acceleration is highest at the time of injection.

The magnetic field that generates the accelerating emf also exerts a centripetal
force that constrains the electrons to a circular path. As the electron velocity
(v) increases, the path radius might also be expected to increase, as in a
cyclotron. However, the magnetic field intensity and hence the centripetal force
is increasing at the same time. By shaping the pole pieces for appropriate adjust-
ment of the field intensity as a function of radial distance, the electron orbits
can be well stabilized.

In theory, the phase interval of the magnetic field waveform during which
electron acceleration can be maintained could continue from the zero crossing
to the point at which the sine wave reaches its peak value. This interval
is 90°. At the peak, although the magnetic field intensity is maximum,
its derivative (i.e., time rate of change) is zero, and, consequently, the

accelerating emf is also zero. If the electrons were permitted to remain within the doughnut after the peak, an emf would appear again but it would be opposite in sign to the accelerating emf and would hence decelerate the particles. Therefore, the phase interval during which acceleration takes place never exceeds 90° and may, in fact, be substantially less, depending on the desired energy level.

The deflection of the electrons from their orbital path to the target may be controlled in either of two ways. As the magnetic field intensity increases, the flux bar saturates, with the result that the radius of the electron path diminishes. The particles then impinge on a target positioned inside of the orbit they traversed while accelerating. Through the use of flux bars with different saturation characteristics, the energy attained by the electrons prior to leaving the acceleration orbit can be predetermined. Alternatively, the electrons can be magnetically deflected from this orbit at any time during the acceleration period by a suddenly applied field. This field is typically generated by the discharge of a condenser into an appropriately positioned coil. This second method obviously provides more options in the placement of the target with respect to the orbit.

From the above description, it is clear that the betatron is a "one shot" machine in the sense that the electrons receive only one accelerating pulse from their initial injection to deflection from the orbit. However, the duration of this pulse is considerable when compared with the time required for an electron to complete a single orbit, so that the particles are continuously accelerated during many orbital revolutions, although at a decreasing rate. For example, a 300 Hz magnetic field has a period (i.e., time required for one complete sinusoidal alternation) of about 3.3 milliseconds. Assuming that the electrons are accelerated during a 90° interval, the actual acceleration time would be 25% (90°/360°) of this, or approximately 0.83 milliseconds. During this brief period, the electrons traverse several tens of thousands of orbits, attaining terminal velocities approaching the speed of light. (An electron accelerated to a moderate kinetic energy level of about

11 MeV would have a velocity greater than 0.999 that of light.) It should be recalled, however, that the electrons as initially injected into the doughnut have already attained considerable velocity. For example, an electron injected with a kinetic energy of 100 keV will be moving at nearly 0.6 light speed before it is further accelerated by the betatron.

2.3 Isotope Production

Radionuclide Production - General Principles

Artificial (i.e., man-made) radionuclides are produced in four different ways:

a. Fission

The fissioning of uranium and plutonium in nuclear reactors results in a number of fission-product isotopes, both stable and radioactive. Among the latter are ^{144}Ce, ^{90}Sr and ^{137}Cs.

b. Neutron Irradiation

An appropriate target is bombarded by neutrons, typically in a reactor. Typical products include ^{32}P (from ^{32}S), ^{14}C (from ^{14}N) and ^{47}Ca (from ^{46}Ca).

c. Accelerators

An appropriate target is bombarded by positively charged particles. Cyclotrons are generally employed. Typical products include ^{129}Cs (from ^{127}I), ^{62}Zn (from ^{60}Ni) and ^{52}Fe (from ^{50}Cr).

d. Radioisotope Generators

An artificial radioisotope generator (cow) spontaneously decays to a desired daughter radionuclide. If the half-life of the cow is sufficiently long, the daughter nuclide can be "milked" as required. In terms of medical application, a generator of particular interest provides ^{99m}Tc from ^{99}Mo. (The "m" means metastable and indicates in this case that ^{99m}Tc has a relatively brief half-life, actually about 6 hours, decaying to ^{99}Tc).

In general, nuclides that are transmuted to radionuclides by bombardment are converted to an unstable state of either (a) proton excess with respect to the number of neutrons in the bombarded nucleus, or (b) neutron excess with respect

to the number of protons. As the bombarding particle is incorporated within the nucleus, other particles or gamma radiation is emitted. In the case of neutron bombardment, a common nuclear reaction is one in which the neutron is "captured" by the nucleus with the concurrent emission of a gamma ray. As a consequence, the atomic mass number of the target nucleus is increased by one, but its chemical identity remains the same.

A simple reaction illustrating this process is:

$$^{27}\text{Al} + \text{neutron becomes } ^{28}\text{Al and a gamma ray is emitted}$$
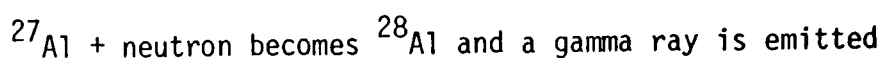
Note that the Al has not been transmuted to some other element; its atomic number remains the same (13) because it has neither gained nor lost nuclear charge. However, its atomic mass has increased from 27 to 28 because of the captured neutron. ^{28}Al is not a stable isotope. The nucleus emits an electron, becoming ^{28}Si. ^{28}Si is stable and has an atomic number of 14 in consequence of the unit increase in nuclear charge. Not all neutron-induced nuclear reactions necessarily result in the formation of radioactive isotopes. For example, if ^{10}B is bombarded by neutrons, ^{7}Li is formed and alpha particles are emitted. This is the "neutron-alpha reaction." ^{7}Li is stable.

Radionuclides produced by accelerators are always formed by positively charged particle bombardment. The "projectiles" used may be protons, deuterons or alpha particles. Depending on the conditions (i.e., identity of target, nature of particle, etc.), any of a number of nuclear reactions may occur. The following is a list of some of the more important of these reactions in terms of the incident particle and the emitted particle or radiation.

Nuclear Reactions Caused by Positive Particle Bombardment

Incident Particle	Emissions
Proton	Deuteron
	Alpha particle
	Neutron
	Gamma ray

Deuteron	Proton
	Alpha particle
	Neutron
Alpha particle	Proton
	Neutron

A standardized form of representation has been developed for symbolizing nuclear reactions such as those categorized above. As an illustration, if ^{12}C is bombarded with deuterons it is transmuted to ^{13}N and a neutron is emitted for each deuteron absorbed. This would be written as

$$^{12}C(d,n)^{13}N$$
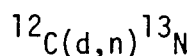
Note that the bombarded nuclide is shown first with its mass number. Within the parentheses are shown the bombarding and emitted entities in that order, separated by a comma. The nuclide resulting from the reaction is shown last, also with its mass number identified. It is usual to omit the atomic numbers (not shown) from these nuclear reaction equations because these numbers are inherent in the identity of the nuclides (i.e., all carbon atoms, for example, regardless of their mass numbers, have the same atomic number - 6).

In the reaction shown above, it can be seen that both the atomic mass and the atomic number have increased by one (that is, the atomic mass change is from 12 to 13 and the change in atomic number is from 6 to 7). This is to be expected because the deuteron consists of one proton and one neutron. Since a neutron is emitted, the net effect is that of the addition of a proton to the bombarded carbon nucleus with a consequent gain of one unit of atomic mass as well as of charge. The resulting ^{13}N is unstable. It emits positrons and has a half-life of only 10 minutes. As another example,

$$^{55}Mn(p,4n)^{52}Fe$$
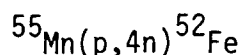
Since, in this reaction, for each proton absorbed there are four neutrons emitted, there is a net loss of three mass units per nucleus, but a gain of one unit of charge.

An illustration of alpha particle bombardment is seen in the production of ^{28}Mg from ^{27}Al. For each interaction of a ^{27}Al nucleus with an alpha particle, three protons are emitted. This is represented as follows:

$$^{27}Al(\alpha,3p)^{28}Mg$$
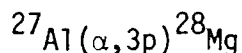
Remembering that an alpha particle consists of two protons and two neutrons, it follows that the atomic mass has increased by one. On the other hand, the nuclear charge has decreased by one (two protons gained, three lost), so that the atomic number has dropped from 13 (Al) to 12 (Mg).

A final example is presented here to demonstrate the possibility of a change in atomic mass without a concurrent change in atomic number. If ^{84}Kr is bombarded with deuterons, one proton is lost for each deuteron absorbed as follows:

$$^{84}Kr(d,p)^{85m}Kr$$
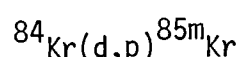
This is the equivalent of adding one neutron to the nucleus, so that there is a gain of one unit of atomic mass with no change in atomic number. The letter "m" following the mass number of 85 means that the product nucleus is a metastable form of ^{85}Kr, with a short half-life. ^{85m}Kr is a beta and gamma ray emitter with a half-life of 4.4 hours. For comparison, non-metastable ^{85}Kr has a half-life of over 10 years.

Radionuclide Production - Methods

The cyclotron is by far the most commonly used accelerator in radionuclide production, although Van de Graaff generators and Cockcroft-Walton machines are occasionally used. In the discussion of linacs presented earlier in this report, it was mentioned that while these devices were originally developed for electron acceleration, they have recently also been used for positive particle acceleration.

The kinetic energies to which the bombarding particles are raised are usually moderate in terms of the capabilities of very large machines. They are typically in the range of 10-30 MeV, with the exact values determined by the identities of the accelerated particles, the target material, and the desired nuclear reaction.

Although the basic principles of radionuclide production by accelerators appear simple, their actual implementation may pose many practical difficulties. For example, the bombardment of the target produces considerable heat which can

rapidly deform, fuse, or even vaporize the target. For this reason, water cooling is generally employed. Furthermore, the target material may be a metal foil, powder, liquid, or even a gas; each of these forms imposes its own particular requirements. To a considerable extent, success in the production of many radionuclides has been due to the ingenuity exercised in the mechanical design of the target structure.

The radionuclide yields practicably attainable with accelerators are lower than those that can be achieved by neutron bombardment, and, therefore, accelerator-produced isotopes tend to be more expensive than those produced in reactors. Accelerator production does, however, have certain general advantages. For example, if the desired radionuclide has a short half-life, such as a few hours, it must be produced at or near the site of use. Further, in some cases it may not be practical to obtain a specific desired radionuclide except by positive particle bombardment.

After the target has been irradiated, the extraction of the produced radionuclide may be simple or complex. In some cases, a salt may be dissolved directly in water. Other procedures, such as precipitation, elution, ion exchange, or chemical separation, may be necessary. The methods used are essentially the same as those used in the processing of radionuclides produced through neutron bombardment.

Radionuclide Production - Specific Examples

As Table 2-1 suggests, the number of medically useful radionuclides is considerable. Actually, the examples shown are by no means comprehensive. Other isotopes of medical interest include ^{11}C, ^{13}N, ^{15}O, ^{43}K, ^{128}Ba, and ^{77}Br, to name a few. The variety of these radionuclides precludes discussion of each, but the technical considerations associated with specific isotopes of particular importance are summarized below.

TABLE 2-1. Radionuclides of Medical Interest

USE	NUCLIDE	FORM	TREATMENT/STUDY	USUAL DOSE	STATE
In vivo	Technetium 99^m	Medronate	Bone Imaging	to 15 mCi	liquid
In vivo	Technetium 99^m	Pertechnetate	Brain Imaging	to 15 mCi	liquid
In vivo	Technetium 99^m	Pertechnetate	Thyroid Imaging	to 2 mCi	liquid
In vivo	Technetium 99^m	Pertechnetate	Blood pool imaging	to 15 mCi	liquid
In vivo	Technetium 99^m	Pertechnetate	Salivary gland imagine	to 2 mCi	liquid
In vivo	Technetium 99^m	Pertechnetate	Placenta localization	to 1 mCi	liquid
In vivo	Technetium 99^m	Stannous polyphosphate	Bone Imaging	to 15 mCi	liquid
In vivo	Technetium 99^m	Sulfur colloid	Liver/spleen imaging	to 3 mCi	suspension
In vivo	Technetium 99^m	DTPA (iron-ascorbate)	Kidney imaging	to 5 mCi	liquid
In vivo	Technetium 99^m	DTPA (tin)	Renal function	to 10 mCi	liquid
In vivo	Technetium 99^m	DTPA (tin)	Kidney imaging	to 10 mCi	liquid
In vivo	Technetium 99^m	DTPA (tin)	Brain imaging	to 15 mCi	liquid
In vivo	Technetium 99^m	HSA microspheres	Lung imaging	to 4 mCi	liquid
In vivo	Technetium 99^m	Disodium etidronate (tin)	Bone imaging	to 15 mCi	liquid
In vivo	Technetium 99^m	Labelled macroalbumin (tin)	Lung imaging	to 4 mCi	liquid
In vitro	Iodine 125, 131	Iodide	Thyroid function	5-25 μCi	liquid
In vitro	Iodine 125, 131	Labelled HSA	Blood volume	to 20 μCi	liquid
In vitro	Iodine 125, 131	Labelled renal function compounds	Renal function	20-50 μCi	liquid
In vitro	Iodine 125, 131	Labelled fats, fatty acids	Fat absorption	25-100 μCi	liquid
In vivo	Iodine 123	Iodide	Thyroid function	100 μCi	capsule
In vivo	Iodine 123	Iodide	Thyroid imaging	400 μCi	capsule
In vivo	Iodine 125,131	Iodide	Thyroid function	5-25 μCi	liq/capsule
In vivo	Iodine 131	Iodide	Thyroid imaging	to 100μCi	liq/capsule
In vivo	Iodine 131	Labelled HSA	Brain tumor localization	to 500 μCi	liquid
In vivo	Iodine 131	Labelled HSA	Placenta localization	5 μCi	liquid
In vivo	Iodine 131	Labelled HSA	Cardiac imaging	to 100 μCi	liquid
In vivo	Iodine 131	Labelled HSA	Cisternography	70-100 μCi	liquid
In vivo	Iodine 125,131	Rose Bengal	Liver function	20-50 μCi	liquid
In vivo	Iodine 131	Rose Bengal	Liver imaging	to 300 μCi	liquid
In vivo	Iodine 125,131	Renal function compounds	Renal function	20-50 μCi	liquid
In vivo	Iodine 131	Renal function compounds	Kidney imaging	100 μCi	liquid
In vivo	Iodine 131	Sodium iodipamide	Cardiac imaging	300-500 μCi	liquid
In vivo	Iodine 131	Labelled macroalbumin	Lung imaging	to 300 μCi	liquid
In vivo	Iodine 131	Labelled microalbumin	Liver imaging	to 300 μCi	liquid
Internal therapy	Iodine 131	Iodide	Hyperthyroidism	5-15 mCi/dose 30-50 mCi/course	liq/capsule "
Internal therapy	Iodine 131	Iodide	Cardiac dysfunction	5-15 mCi/dose 30-40 mCi/course	liq/capsule "
Internal therapy	Iodine 131	Iodide	Thyroid cancer	to 100 mCi/dose 300-400 mCi/course	" '

Table 2-1 (Continued)

USE	NUCLIDE	FORM	TREATMENT/STUDY	USUAL DOSE	STATE
Internal therapy	Iodine 131	Iodide	Thyroid ablation	50-100 mCi	liq/capsule
In vivo	Xenon 133	Gas in saline	Cardiac abnormalities	to 50 mCi	gas in liq
In vivo	Xenon 133	Gas in saline	Muscle blood flow	to 200 μCi	gas in liq
In vivo	Xenon 133	Gas in saline	Cerebral blood flow	to 1 mCi	gas in liq
In vivo	Xenon 133	Gas	Pulmonary function	to 10 mCi	gas
In vitro	Chromium 51	Chromate	RBC mass/survival	to 200μCi	liquid
In vitro	Chromium 51	Labelled HSA	GI protein loss	to 50 μCi	liquid
In vivo	Chromium 51	Chromate	Spleen imaging	to 300 μCi	liquid
In vivo	Chromium 51	Chromate	Placenta localization	10 μCi	liquid
In vivo	Chromium 51	Chromate	Red cell sequestration	to 200 μCi	liquid
In vivo	Chromium 51	Labelled HSA	Placenta localization	5-35 μCi	liquid
In vitro	Cobalt 57, 58, 60	Labelled vitamin B12	B 12 absorption	0.5 μCi	liquid
In vivo	Fluorine 18	Fluoride in saline	Bone cancer imaging	to 4 mCi	liquid
In vivo	Gallium 67	Citrate	Tumor localization	to 4 mCi	liquid
In vivo	Gold 198	Colloid	Liver imaging	to 200 μCi	suspension
Internal therapy	Gold 198	Colloidal	Pleural effusions	to 125 mCi	suspension
Internal therapy	Gold 198	Colloidal	Peritoneal effusions	to 200 mCi	suspension
In vitro	Iron 59	Citrate, chloride, sulfate	Iron turnover	10-35 μCi	liquid
In vivo	Iron 59	Citrate, chloride, sulfate	Iron distribution	10-35 μCi	liquid
In vivo	Indium 111	DTPA	Cisternography	500 μCi	liquid
In vivo	Krypton 81^m	Gas	Pulmonary function	3 mCi	gas
Internal therapy	Phosphorus 32	Soluble phosphate	Polycythemia vera	3-7 mCi/dose 8-10 mCi/course	liquid "
Internal therapy	Phosphorus 32	Soluble phosphate	Leukemia	1 mCi/dose 8-10 mCi/course	liquid "
Internal therapy	Phosphorus 32	Soluble phosphate	Osseous metastases	1.25 mCi/dose 20 mCi/course	liquid "
Internal therapy	Phosphorus 32	Colloidal chromic phosphate	Pleural effusions	to 20 mCi	suspension
Internal therapy	Phosphorus 32	Colloidal chromic phosphate	Peritoneal effusions	to 25 mCi	suspension
In vivo	Selenium 75	Labelled methionine	Pancreas imaging	to 250 μCi	liquid
In vivo	Strontium 85	Nitrate, chloride	Bone cancer imaging	50-100 μCi	liquid
In vivo	Thallium 201	Chloride	Cardiac imaging	to 1.5 mCi	liquid
In vivo	Ytterbium 169	DTPA	Cisternography	500 μCi	liquid

● ^{123}I

Although ^{131}I has a long history of use in thyroid function studies and in thyroid imaging, ^{123}I offers several distinct advantages which account for the growing interest in this isotope.

These are:

a) Half-life $(T_{1/2})$

The half-life of ^{123}I is about 13 hours as opposed to that of ^{131}I which is approximately 8 days. The shorter $T_{1/2}$ reduces cumulative patient exposure.

b) Gamma ray energy

The principal photonic emissions of ^{123}I have energies of 159 KeV. This level is consistent with the spectral response of current gamma cameras. The equivalent energies of ^{131}I photons are about 364 keV.

c) Beta radiation

^{131}I emits abundant beta radiation which serves no medically useful purpose in vivo but contributes to patient exposure. ^{123}I is free of significant beta emission.

^{123}I is generated by either of two methods:

a) Bombardment of antimony or tellurium

In one procedure, ^{121}Sb is bombarded with alpha particles, with a consequent emission of two neutrons for each alpha particle absorbed, as follows:

$$^{121}Sb(\alpha,2n)^{123}I$$
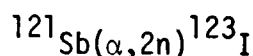
Both the mass and atomic numbers increase by two units in this reaction. In another procedure, ^{123}Te is bombarded with protons, with a consequent emission of one neutron per absorbed proton. The reaction is

$$^{123}Te(p,n)^{123}I$$
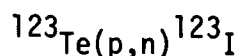
The atomic mass remains the same, but the atomic number increases by one.

b) As a decay product of ^{123}Xe

^{123}Xe can be produced by bombarding ^{122}Te with alpha particles according to the reaction

$$^{122}Te(\alpha,3n)^{123}Xe$$
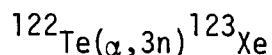
^{123}Xe is unstable, having a half-life of slightly over 2 hours. It decays by positron emission (one positron per nucleus) with a consequent drop in atomic number from 54 to 53.

● ^{99m}Tc

This radionuclide has a half-life of slightly over 6 hours. Its principal radiation - gamma rays - has an energy level of about 140 keV, which is excellent for imaging purposes. Reference to Table 2-1 will show that ^{99m}Tc is used for visualizing a wide variety of organs and tissues. At present, ^{99m}Tc is used more extensively than any other isotope in imaging procedures.

As previously mentioned, ^{99m}Tc is now produced mainly in radioisotope generators in which the cow is ^{99}Mo. ^{99}Mo itself is generally made either by fission or neutron bombardment of ^{98}Mo. In recent years, however, there have been studies addressing the feasibility of generating ^{99m}Tc using accelerators. It appears that this can be achieved through protron bombardment of ^{100}Mo. In this reaction two neutrons are lost per nucleus, so that the mass number decreases by one, while the atomic number increases by one (i.e., 100 to 99 and 42 to 43), as is shown in the following:

$$^{100}Mo(p,2n)^{99m}Tc$$
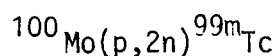
The possibility of producing ^{99}Mo cow in accelerators has also been explored. This can be accomplished by bombarding ^{100}Mo with protons. The resulting reaction is

$$^{100}Mo(p,p\,n)^{99}Mo$$
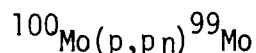
As is clear from the above, the net effect of the bombardment is a drop in atomic mass of one unit with no change in atomic number.

2.4 <u>Applications</u>

This section focuses on radionuclide labeled compounds of medical interest.
The applications of these materials fall into two broad categories:

- <u>in vivo</u> (within the living organism)

    Labeled materials designed for clinical application are generally
    administered orally or by injection. Their principal uses are:
    (a) imaging; (b) function studies; and (c) therapy. Such materials
    are "radiopharmaceuticals." Labeled compounds are also to be used
    <u>in vivo</u> for medical or biological research purposes as distinguished
    from clinical diagnosis or treatment.

- <u>in vitro</u> (in an artificial environment - literally "in glass")

    This class spans a wide gamut of clinical laboratory tests and
    analyses in which labeled compounds are employed as reagents.*

Detailed treatment of the medical applications of radionuclide labeled com-
pounds is outside of the scope of this report. However, the following
summary provides a general orientation.

a) Imaging

    As the name suggests, imaging is a procedure for enabling the visual
    examination of internal structures or functions. In a sense, it is the
    reverse of conventional X-ray techniques in which an <u>external</u> source of
    radiation is differentially transmitted through anatomic structures
    on the basis of their different densities. In imaging, gamma-emitting
    radionuclides incorporated in appropriate compounds may be selectively
    absorbed by or become bound by the organ or tissue being
    examined. For example, in the case of bone, the labeled compound would
    be a phosphate. In other imaging procedures, the radionuclide may be
    introduced into a body fluid (e.g., blood, cerebrospinal fluid) for
    such purposes as delineating some portion of the cardiovascular system
    or the ventricles of the brain. A considerable amount of imaging is

---

*The distinction between radiopharmaceuticals and labeled laboratory reagents
 is evident. For convenience, however, the term "radiopharmaceutical industry"
 is sometimes used as including the manufacture and distribution of <u>all</u> types
 of labeled materials designed for medical and related uses.

performed by scanning techniques in which a detector (typically, a crystal that scintillates when excited by gamma radiation of appropriate energy level) is progressively moved in steps across the area to be imaged. The generated presentation is thus a composite or mosaic composed of many individual elements. With other techniques, using a large stationary crystal, it is possible to photograph the radiation from a given area simultaneously (gamma ray camera). In this case, however, the size of the field that can be observed at one time is limited by the dimensions of the crystal. Scanning methods are useful when the structure to be visualized is large and static. The imaging of dynamic processes, such as blood flow, obviously requires simultaneous area photography. The principal purpose of imaging is to detect and identify abnormalities, such as malignancy, vascular defects (e.g., aneurism or stenosis), and other pathologic changes.

b) Function Studies

These studies are performed for the purpose of assessing the physiological or biochemical activity of the organ or tissue of interest. Such studies are performed essentially in vivo and include respiratory exchange, blood volume measurements, gastro-intestinal protein loss, vitamin B_{12} absorption, iron metabolism and thyroid activity as measured by ^{131}I uptake.

c) Therapy

Compounds containing radionuclides are used in vivo for various therapeutic purposes, including the treatment of metastatic bone tumors, thyroid hyperfunction and malignancy, and polycythemia vera (excessive red blood cell count). Where applicable, in vivo radiotherapy is considered to have an advantage over irradiation from an external source in that the former is more selectively directed with consequently less damage to normal tissues adjacent to the treated site.

The number of isotopes that have been and are being used for medical purposes and the variety of these uses are considerable. Table 2-1 lists several examples of commonly used radionuclides and their applications, both in vivo and in vitro. Note that in some instances the nuclides are used as tags or labels, as in the case of iodine, while in others they are used in elemental form (e.g., ^{81m}Kr).

3.0 EXTENT OF ACCLERATOR USE IN UNITED STATES

3.1 Growth in Accelerator Use

Estimates of the number of particle accelerators by states in the United **States** are published in the report of State and Local Radiological Health Programs[1] by the Food and Drug Administration, Bureau of Radiological Health (BRH). These data have been reported annually and were obtained for the years 1968 and 1970-1977. For the most part, the states exclude Federally owned machines.*

In many cases, data are missing due to failure of some of the states to respond to the BRH questionnaire, upon which the report is based. These missing data have been developed to the extent possible by using data from previous and subsequent years to interpolate to the year of interest. In some cases, we asked the state for the missing data.

The estimated number of particle accelerators in the United States reported to BRH for the years 1968-1977 and the adjusted totals are shown in Table 3-1; a breakdown by state is in Table 3-2. The adjusted totals for these years are plotted in Figure 3-1. A least squares linear regression analysis was performed on the data to obtain the growth curve shown in the figure. For such a curve it is desirable to know how well the linear curve actually fits the data; this measure is defined as the correlation coefficient. For this curve, it was determined to be 0.99. A linear growth rate of 65 accelerators per year was obtained from which the number of particle accelerators can be projected:

      1980 - 1355 machines
      1981 - 1420 machines
      1982 - 1485 machines
      1983 - 1550 machines

---

*BRH defines accelerators to include machines producing electrons greater than 300 keV or ions greater than 150 keV.

TABLE 3-1

PARTICLE ACCELERATORS IN THE U.S.

YEAR	TOTAL NUMBER REPORTED [1]	ADJUSTED TOTAL*
1968	576	600
1969	N/A	625
1970	639	650
1971	790	790
1972	714	845
1973	875	877
1974	963	965
1975	833	1029
1976	845	1055
1977	1113	1191

*Total reported plus number of additional machines obtained by extrapolation and by direct contact with states.
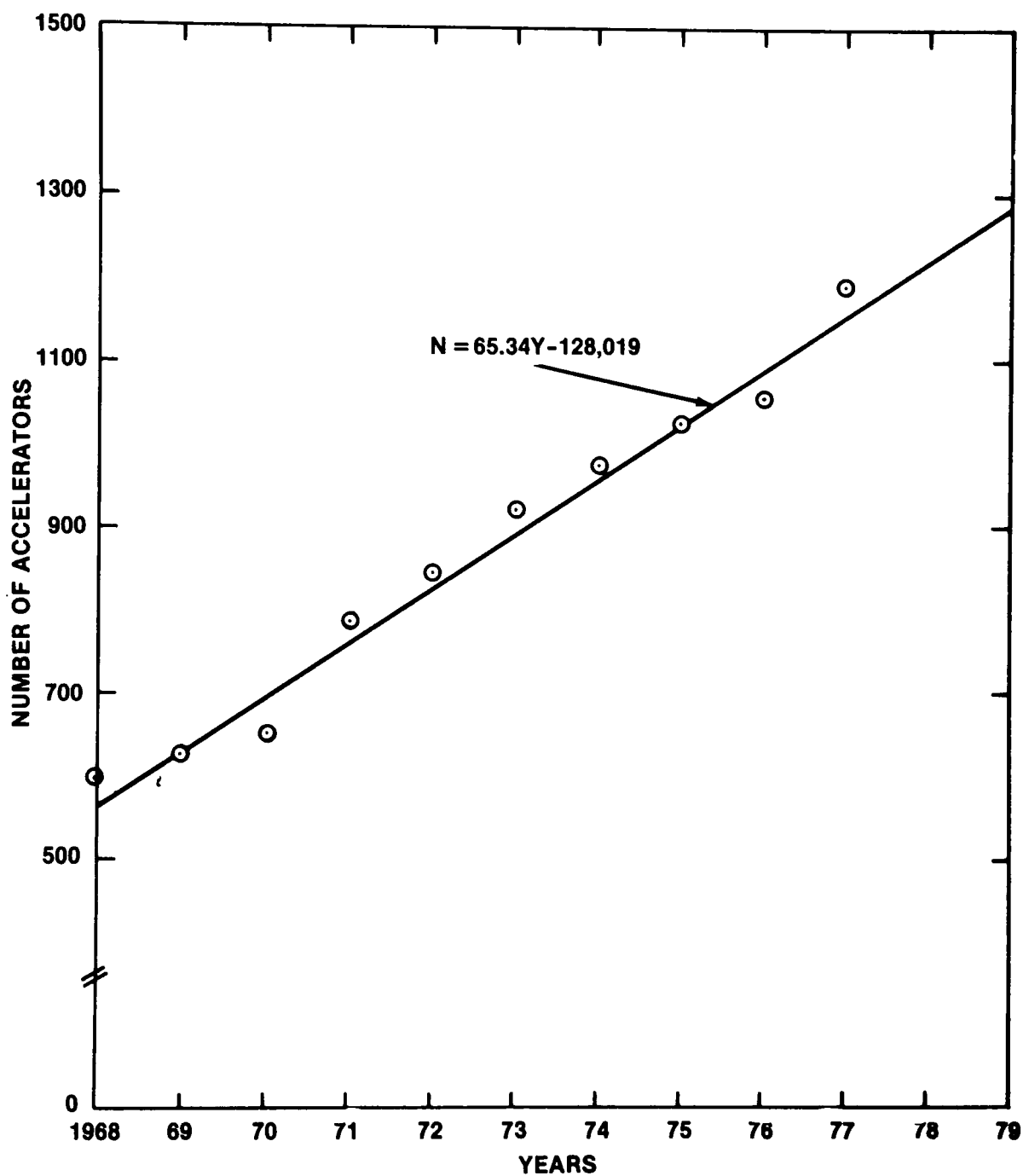
FIGURE 3-1
GROWTH TREND OF PARTICLE ACCELERATORS IN THE UNITED STATES

3-4

TABLE 3-2

ADJUSTED ESTIMATES OF PARTICLE
ACCELERATORS BY STATE - 1977

State	Number of Accelerators	Number Registered	Number of Users
Total	1191	982	825
Alabama	24	18	59
Alaska	NA	NA	NA
Arizona	36	13	8
Arkansas	7	5	5
California	177	177	85
Colorado	12	7	7
Connecticut	13	10	10
Delaware	7	3	7
District of Columbia	10	10	10
Florida	59	59	38
Georgia	21	21	15
Hawaii	2	2	2
Idaho	2	NA	2
Illinois	57	57	41
Indiana	26	33	33
Iowa	NA	NA	NA
Kansas	10	10	6
Kentucky	10	10	8
Louisiana	15	18	14
Maine	0	0	0
Maryland	26	26	NA
Massachusetts	33	33	33
Michigan	57	57	NA
Minnesota	7	7	11
Mississippi	11	11	7
Missouri	11	11	6
Montana	2	2	2
Nebraska	8	5	6
Nevada	6	NA	NA
New Hampshire	3	3	3
New Jersey	31	31	19
New Mexico	4	4	4

NA - Data not available

TABLE 3-2 (continued)

ADJUSTED ESTIMATES OF PARTICLE

ACCELERATORS BY STATE - 1977

State	Number of Accelerators	Number Registered	Number of Users
New York	121	0	66
North Carolina	7	13	5
North Dakota	1	1	1
Ohio	30	23	23
Oklahoma	13	13	13
Oregon	19	19	19
Pennsylvania	83	69	67
Rhode Island	5	5	2
South Carolina	51	36	13
South Dakota	NA	NA	NA
Tennessee	25	25	18
Texas	75	70	95
Utah	5	NA	5
Vermont	NA	NA	NA
Virginia	11	8	8
Washington	26	26	26
West Virginia	6	6	6
Wisconsin	22	22	15
Wyoming	1	NA	1
Puerto Rico	3	2	1

NA - Data not available

3.2 Use by Type of Machine

The annual BRH reports, discussed above, do not break down accelerator use
by type of machine. However, the questionnaire BRH distributes to obtain the
use data asks for such a breakdown. The responses to the 1977 questionnaire
in the area of accelerator use were made available to Teknekron. These re-
sponses were compiled into the seven categories of accelerators found in
the questionnaire. The results are presented in Figure 3-2, which clearly
shows that linacs are the most widely used machine.

This trend is largely due to the increasingly wide use of linacs in the medical
therapy field. A BRH report on electron linacs in medical radiation therapy[2]
indicates that these machines are replacing teletherapy sources (e.g., cobalt-60)
that require periodic replacement due to radioactive decay, and older medical
therapy accelerators (e.g., Van de Graaffs, resonant transformers). This
report estimates a 15% per year growth in medical linacs, and projects 400 to
450 such machines in use in 1977 (see Figure 3-3). The present study estimates
that 590 linacs (all types) were in use in 1977, and about 70% of them (or 420)
were used in medical applications.

The growth of medical linacs at the rate of 15% per year is expected
to continue through 1980.[2] There is a basis for projections beyond 1980
since the market for these machines is far from saturated and includes hospitals
and clinics currently operating cobalt-60 units and those considering the
purchase of a megavoltage therapy unit. The total number of machines reported
by type is 870, or 73% of the estimated total in 1977. We can see no bias in
the results and assume that the remaining 27% of the machines are distributed
in the same way. However, data obtained from accelerator industry sources[3]
indicate that about 400 Cockcroft-Walton type machines are in use as ion
implanters.* Most of these machines should appear in the "other" category in
Figure 3-2, which shows only 25 machines. Ion implanters are either unregistered

*Ion implanters are used in the semi-conductor industry to implant ions in
 silicon and germanium.

or greatly underreported by many states. Because of their design and low energy (∿0.2MeV), ion implanters do not create airborne radioactivity, so this anomaly was not investigated further.

While implantation is the most popular application of industrial accelerators,[3a] other applications include industrial radiography (X-ray and neutron generators), analysis of materials food processing and sterilization, and curing of coatings and paint. Most X-ray generators used for industrial radiography are not included in our count of accelerators because most fall below the energy cutoff of 300 keV (electrons). Since their average potential is 150 kVp, only a small fraction of the estimated 3300 radiographic X-ray generators are electron accelerators of greater than 300 keV.[3a]

FIGURE 3-2
ACCELERATORS REPORTED BY TYPE
(From BRH Questionnaire)

PERCENT OF TOTAL BY ACCELERATOR TYPE
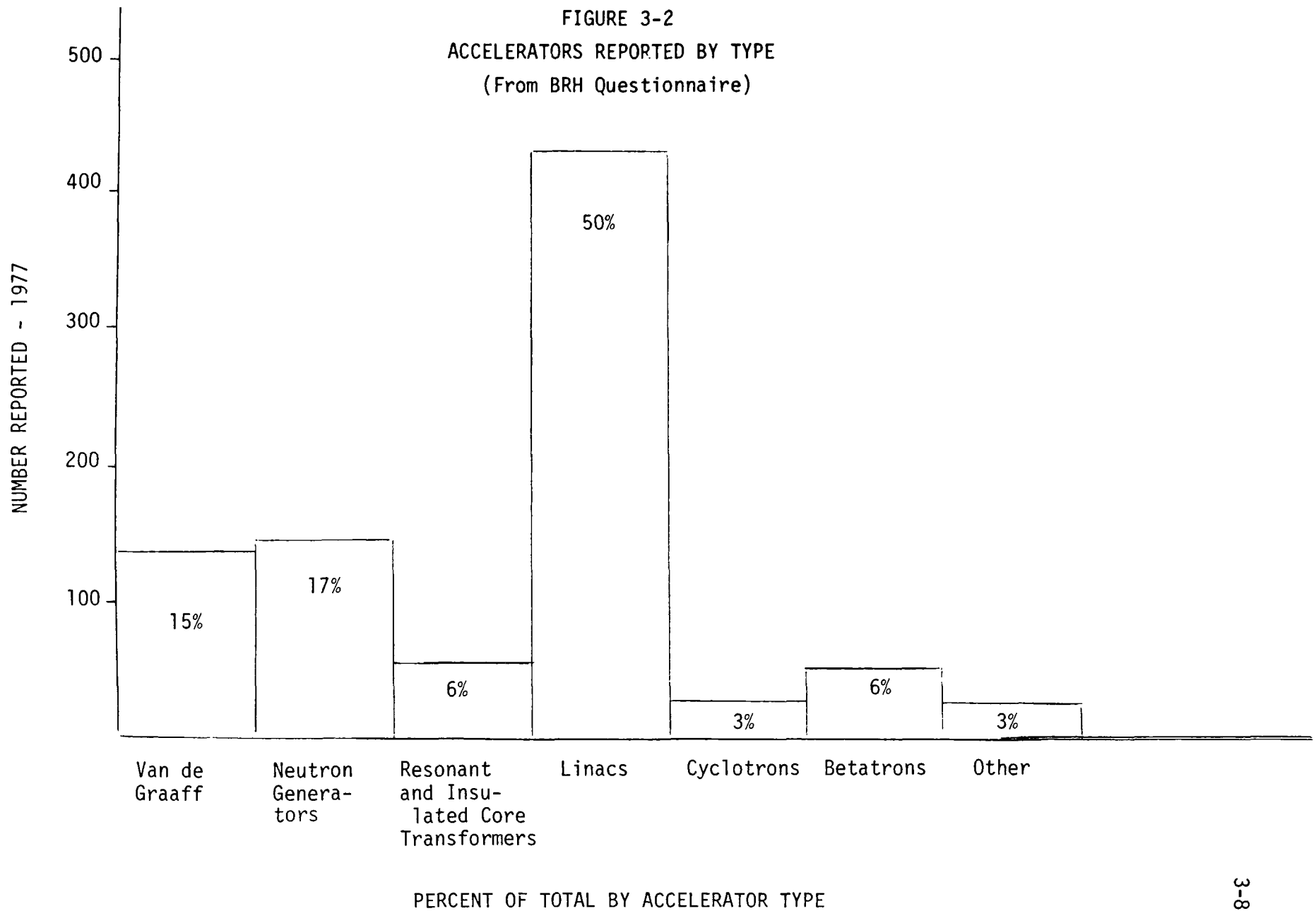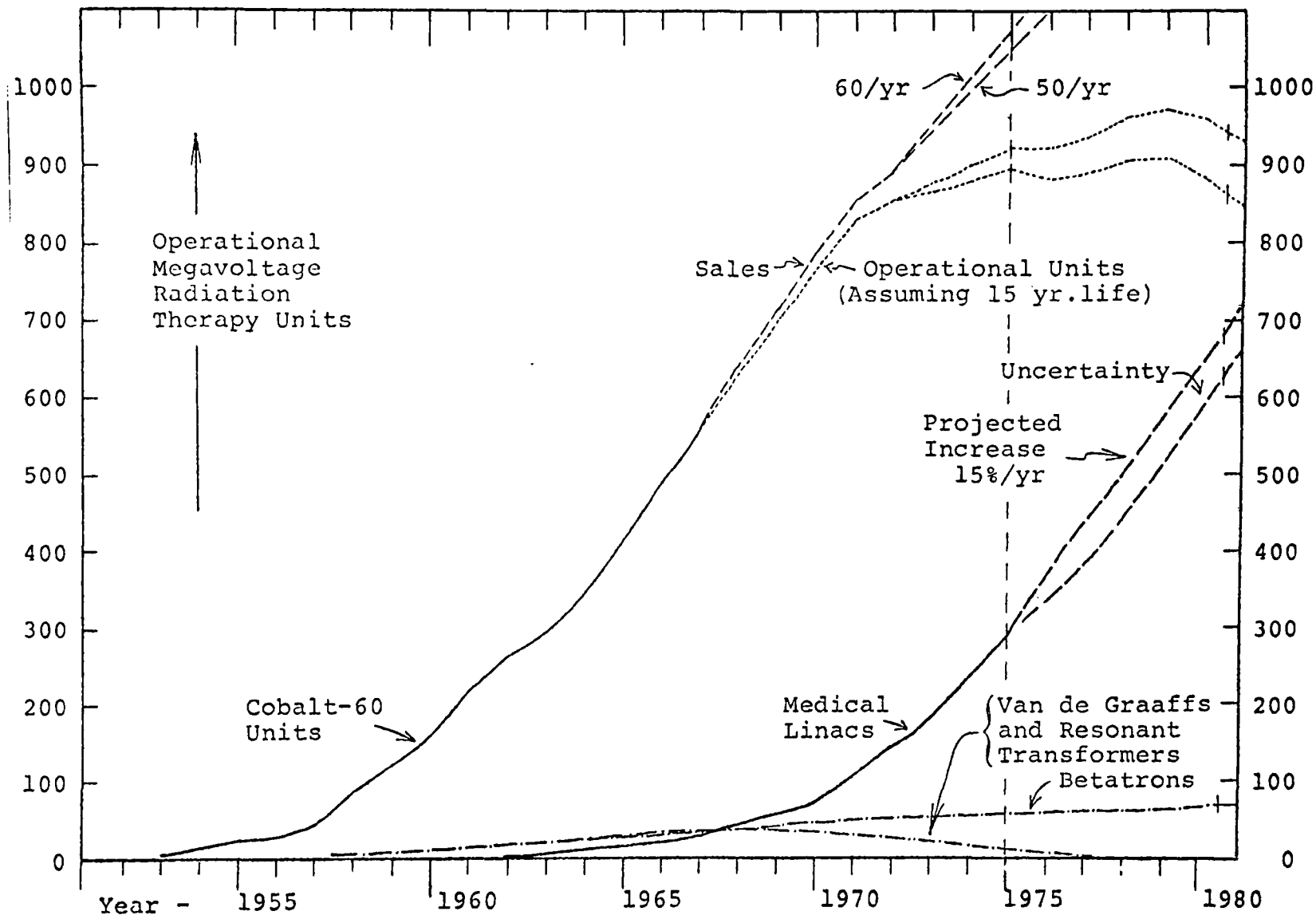
FIGURE 3-3

MEGAVOLTAGE RADIATION THERAPY EQUIPMENT PROJECTIONS FOR THE
UNITED STATES THROUGH 1980[2]

Additional sources of data on accelerator use were found in the American
Institute of Physics (AIP) Handbooks. The first and second editions [4,5] of
the handbooks contain listings of all U.S. accelerators for the years 1955
and 1960, including location, operator/owner, and machine parameters (e.g.,
energy, particle). The data on non-Federally controlled machines were com-
piled under the same general machine classifications used earlier. However,
the class of "neutron generator" was removed since it is an application
(usually of a Cockcroft-Walton machine) that was not identified in the AIP
listings. In order to obtain current figures for comparison with the data
available from the above sources for 1955 and 1960 and the 1977 BRH study,
Teknekron contacted a number of directors of State Radiological Health Programs.
The information obtained represented a total of 376 machines and provided
their classification by kind, particle type, and energy. The results are
presented in Table 3-3, which also gives similar information from the AIP for
1955 and 1960.

The percentages of the total number of machines by type from this table, in
addition to the same breakdown from the BRH questionnaire (Figure 3-2), are
depicted for comparison in Figure 3-4. The shift away from Van de Graaffs
and cyclotrons and towards linacs is evident from this figure.

3.3 Machine Use by Location

An attempt was made to characterize accelerator use by location. References 4
and 5 were relied on for location data (i.e., city) for the years 1955 and 1960,
while current information was obtained from the Teknekron survey. Of the 129
machines operating in 1955, [4] 44 were classfied by location. The Teknekron
survey yielded location data on 376 machines.

A simple classification scheme was used: urban, suburban, and rural. An
urban area was defined as a city with a population of at least 50,000; a sub-
urban area was defined as a city with a population of at least 30,000 and bor-
dering an urban area. All other locations were considered rural. Having located
the accelerator by city, the location was then classified accordingly.

(a) TEKNEKRON - 1979

Energy MeV	VdG e⁻	VdG *	VdG ion	ICT** e⁻	ICT** *	ICT** ion	Linac e⁻	Linac *	Linac ion	Cyc p	Cyc *	Cyc d	Betatron e⁻	Neutron Generator	C-W e⁻	C-W *	C-W ion
<1	10	3		7			9				2		4	8	5	4	18
1-19	26	23	6	8			134	41	1	2		2	4	14	1		1
20-100	1						4	3		6		2	22				
>100		1								1		3					
Total	-70-			-15-			-192-			-18-			30	-22-	-29-		
% of Total	18.1			4.0			51.1			4.8			8.0	5.9	7.7		

(b) AMERICAN INSTITUTE OF PHYSICS - 1960

Energy MeV	VdG e⁻	VdG photon	VdG ion	ICT e⁻	ICT ion	Linac e⁻	Linac ion	Cyc p	Cyc d	Cyc α	Betatron e⁻	Synch e⁻	Synch p	C-W ion	C-W e⁻
<1			8	1						2				31	
1-19	30	33	50	2		14	1	13	5		1			2	1
20-100						9	2	1		1	27	4			
>100						1	2	6			2	4	2		
Total	-121-			-3-		-29-		-28-			-30-	-10-		-34-	
% of Total	48.5			1.1		11.3		10.8			11.7	3.9		13.2	

(c) AMERICAN INSTITUTE OF PHYSICS - 1955

Energy MeV	VdG e⁻	VdG photon	VdG ion	ICT e⁻	ICT ion	Linac e⁻	Linac ion	Cyc p	Cyc d	Cyc α	Betatron e⁻	Synch e⁻	Synch p	C-W ion	C-W e⁻
<1	1		5			1	1	5	11					13	
1-19	7	9	37			5		1	1	3	1	2			
20-100						1	2				7	7	1		
>100						1		5			3				
Total	-59-			-0-		-11-		-25-			-11-	-10-		-13-	
% of Total	45.7			0		8.5		19.4			8.5	7.7		10.1	

TABLE 3-3

ACCELERATOR USE BY TYPE AND ENERGY

*Particle not specified
**Insulated core transformer

FIGURE 3-4
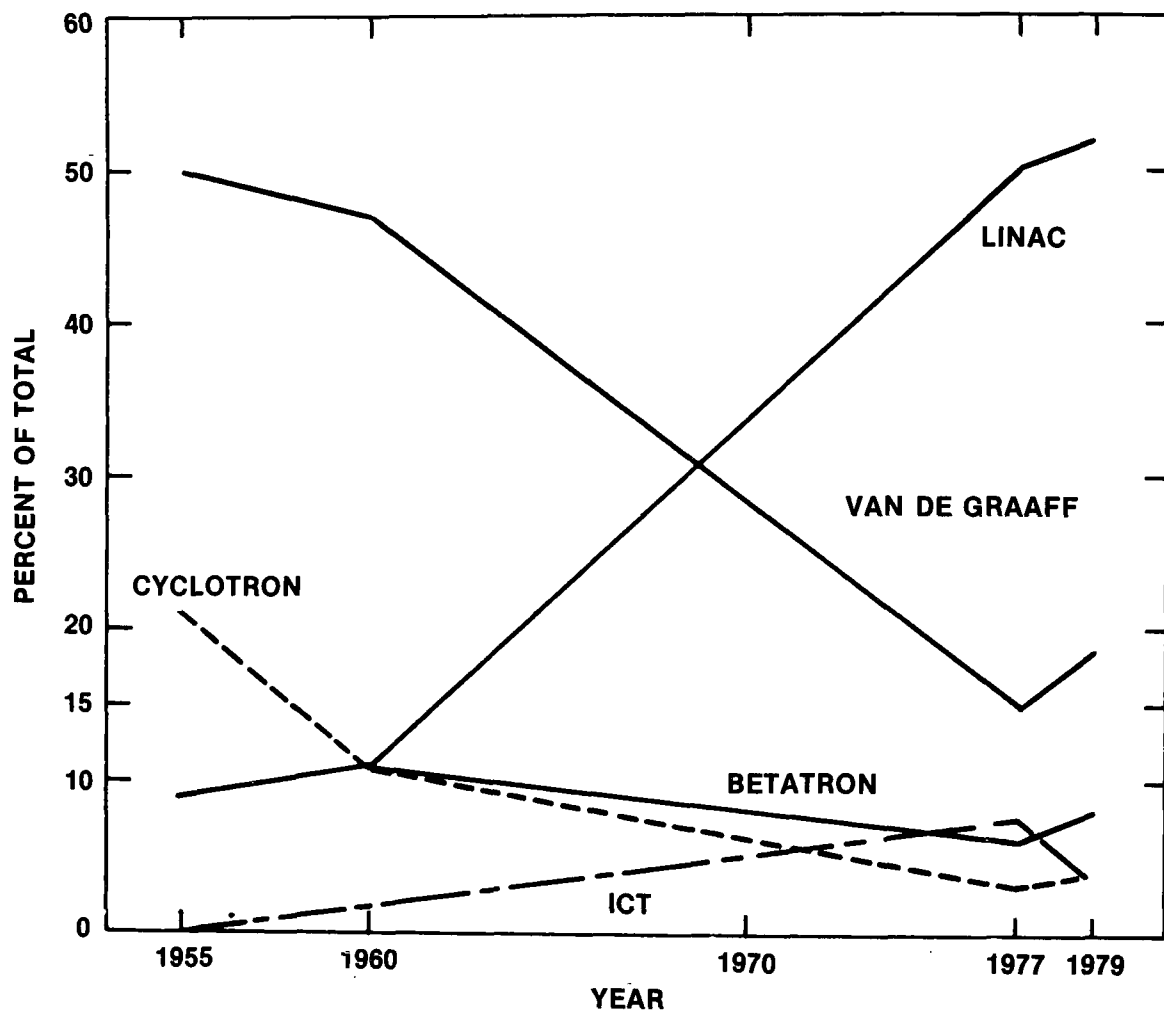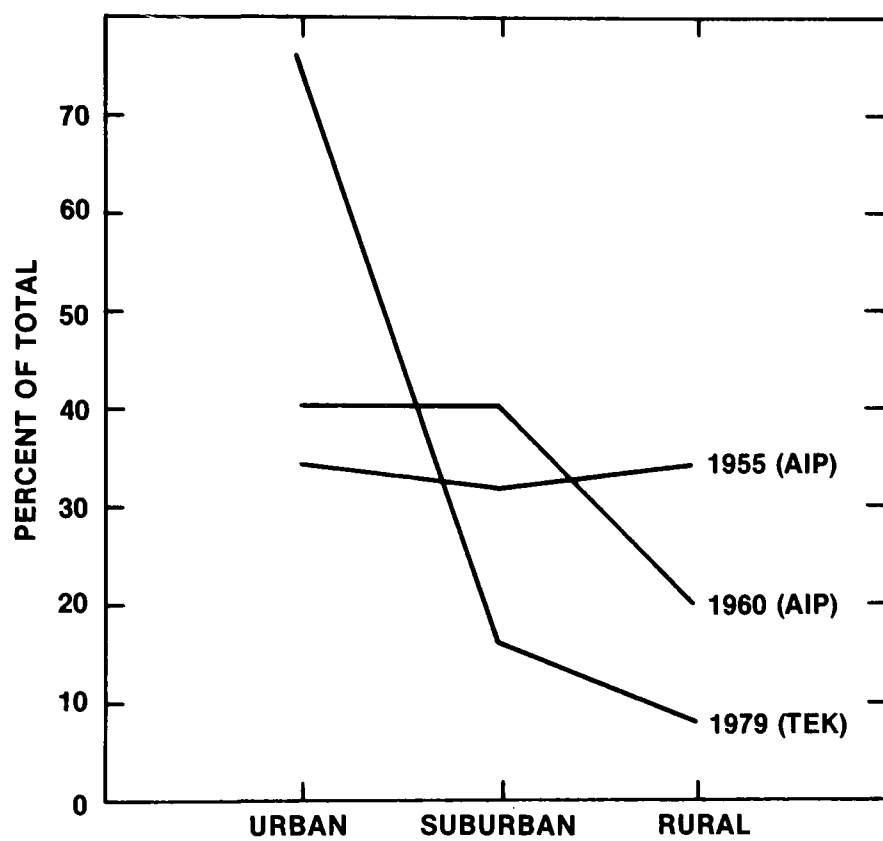**ACCELERATOR USED BY TYPE**

FIGURE 3-5
ACCELERATOR USED BY LOCATION

The results are presented in Figure 3-5 and show a definite trend toward use in urban areas. This is most likely due to the widespread use of linacs as cancer therapy units in urban hospitals, and, to a lesser extent, accelerators being used in commercial applications in urban industrial areas.

4.0 POTENTIAL FOR RESIDUAL AIRBORNE ACTIVITY

4.1 Accelerator Radiation Hazards

Accelerator radiation fields are of two distinct types. The prompt radiation field; produced during the existence of a beam or operation of the accelerator, has the greater energy content, and thus constitutes the greater potential hazard. However, this prompt radiation, from primary and secondary beams and scattered radiation, does not generally present a biological hazard because shielding and exclusion are employed to limit the exposure of radiation workers to allowable levels.

The residual field, remaining after the beam or accelerator is off, is created when the energy of the prompt radiation exceeds the threshold for nuclear reactions. Interactions in materials of the accelerator complex and its contents produce lingering radioactivity with different half-lives and decay radiations. In higher energy accelerators, the exposure of personnel to the activation products in certain machine components, such as target and extraction equipment, constitutes the principal biological hazard from external exposure.

If the primary beam emerges into air before reaching its target, ozone will be produced and, if its energy is sufficient, nuclear reactions with the gas molecules will occur. Since air is composed chiefly of nitrogen and oxygen, the majority of the radioactive products have short half-lives. Radionuclides with lives of less than one minute (e.g., ^{12}N - 0.01 seconds), are not of concern since they are quickly removed by decay. Long-lived activities (e.g., ^{3}H - 12 years) do not constitute a hazard because of their low activity. The principal hazard is exposure to personnel entering the target area immediately after machine shutdown, if area ventilation is inadequate.

4.2 Mechanisms for Air Activation

The most important mechanisms by which radioactivation of air atoms may occur as a consequence of accelerator operation are:

- Direct exposure of air to the primary beam, if the beam passes from the accelerator tube vacuum into the atmosphere, and

- Exposure of air to secondary radiation from the target.

In addition, radioactive gases may be produced within the target and subsequently escape to the local environment (if the target is external to the vacuum); in some instances, the target may contain inherently radioactive material (e.g., tritium). In general, the identities of the radionuclides generated by air activation and their rates of generation depend on several factors, including the type, energy, and intensity of the primary beam and the nature of the target.

Protons and heavy ions accelerated to high energies produce nuclear reactions directly. All energetic accelerated particles give rise to protons and neutrons as secondary radiations from interactions in various targets. Table 4-1 lists the important nuclear reactions initiated in air by protons, neutrons, and photons. Reaction threshold energies and cross sections are also shown.

Table 4-2 lists the products of the above reactions and other nuclides capable of being produced in the particle fluxes near accelerators.

4.3 Calculation of Production Rates

A representative equation useful for the calculation of production rates of airborne radionuclides comes from Patterson and Thomas, p. 520, Equation 12:[6]

$$S = C \sum_i \left[\sum_j \Phi_\gamma \, N_j \, \bar{\sigma}_{ij\gamma} + \sum_j \Phi_{th} N_j \, \bar{\sigma}_{ijth} + \sum_j \Phi_{HE} N_j \, \bar{\sigma}_{ijHE} \right]$$
$$\times \, (1 - e^{-\lambda_i T}) \, e^{-\lambda_i t} \, ,$$

TABLE 4-1

NUCLEAR REACTIONS RESPONSIBLE FOR MOST
AIRBORNE RADIOACTIVITY AROUND ACCELERATORS

Reaction	Parent	Threshold Energy (MeV)	Average Cross Section (millibarns)
(γ,n)	^{14}N	10.5	3*
	^{16}O	15.7	11*
	^{12}C	18.7	10*
$(n,2n)$	^{14}N	11.3	6
	^{16}O	18	40
	^{12}C	20	20
(p,pn)	^{16}O	10	33
	^{14}N	10	10
(n,γ)	^{40}Ar	-	610

*Resonance cross sections at about 22 MeV range from 50-150 mb.

TABLE 4-2

LIST OF AIR ACTIVATION RADIONUCLIDES

Isotope	Half-life	Principal Means of Production
^{15}O	2 min	^{16}O (n,2n), (γ,n) and (p,pn)
^{13}N	10 min	^{14}N (n,2n), (γ,n) and (p,pn)
^{16}N	7 sec	^{16}O (n,p) and ^{15}N (n,γ)
^{14}O	1 min	^{14}N (p,n)
^{11}C	20 min	^{12}C (n,2n) and (γ,n)
^{41}Ar	1.9 hr	^{40}Ar (n,γ)
^{7}Be	53 days	^{12}C (^{3}He, 2α) and others
^{3}H	12 yr	various
^{38}S	37 min	^{40}Ar (γ, 2p) and ^{37}Ci (α, 3p)
^{18}F	2 hr	^{16}O (α,pn) and others

where S   is the total specific activity of radioactive air (per liter),

C   is a constant,

Φ_γ, Φ_{th}, and Φ_{HE} are the average photon, thermal neutron,
and high-energy particle flux densities,

$\bar{\sigma}_{ij\gamma}$, $\bar{\sigma}_{ijth}$ and $\bar{\sigma}_{ijHE}$ are the corresponding average cross sections.

N_j is the number of target nuclei of type j in a liter of atmospheric air,

λ_i is the decay constant of the radionuclide i,
T   is the irradiation time,

and   t   is the decay time.

A simpler equation is found in Barbier, p. 15, Equation 3.8:[7]

n: (specific activity of isotope i produced per unit time) =

$$\Phi \frac{N_o}{A_t} \sigma_{ij} \; (1-e^{-T/t_m}) \; e^{-t/t_m}$$

where N_o is the number of gram-atoms of target material,

A_t is the atomic weight of air (15g),

t_m is the mean life of isotope i, and

other terms are defined as above.

Essentially, the production rates of air activation products are functions of the following factors:

1. the incident flux (ϕ) or secondary flux produced by the accelerator,

2. the density of target gas atoms in the beam path,

3. the appropriate cross section for the reaction and the interaction energy,

4. a buildup factor, based on exposure time, having a maximum in the equilibrium condition, and

5. the decay that occurs between termination of the irradiation and the time of exposure to the decay radiations.

As an example, calculations were performed to estimate the production rates of ^{15}O, ^{13}N, and ^{11}C in the presence of a high-energy neutron flux. The conditions assumed were a 1 μA proton beam striking a thick beryllium target at 100 MeV. According to reference 6, this arrangement produces 2×10^{12} neutrons per second with energies distributed around 100 MeV. Assuming a 1 cm^2 beam traversing 1 meter of air, and using the abundances of C, N, and O isotopes in air, production rates were calculated. They are presented in Table 4-3. Assuming 10 air changes per hour,[19] the total activity produced in 4 hours was also calculated. This is equivalent to the activity released to the atmosphere if it is assumed that activation products are exhausted immediately after production.

TABLE 4-3
PRODUCTION RATES OF ^{15}O, ^{13}N, and ^{11}C IN AIR

Reaction	Production Rate atoms/sec	Amount Produced in 4 hours (Ci)
$^{12}C(n,2n)^{11}C$	6×10^4	7×10^{-5}
$^{14}N(n,2n)^{13}N$	5×10^7	5.3×10^{-2}
$^{16}O(n,2n)^{15}O$	9×10^7	9.4×10^{-2}

An estimate of the thermal neutron flux is not available for this situation; thus production rates of ^{41}Ar and other (n,x) products cannot be calculated. However, it is possible to use the measured thermal flux around an 18 MeV electron linac, a machine widely used in the United States (see Section 3.3). This flux was reported to be about 440 $n/cm^2/sec$.[17] Assuming a 2000-hour work-year, the activity produced annually of ^{41}Ar and ^{14}C in a 27 m^3 room with 10 air changes per hour is 10^{-4} and 10^{-9} curies, respectively.

5.0 EFFLUENT MONITORING DATA

5.1 Existing Data

Of the existing monitoring data reviewed, references 8 and 9 are the most closely related to this study, in that the production of radioactive gases was investigated at three 40 MeV electron linacs operating at up to 0.5 mA. Two linacs[8] were operated with either aluminum targets which produced bremsstrahlung (maximum energy $\sim$20 MeV), or with tungsten targets which produced photoneutrons.

Full power (25 kW) operation with a tungsten target produced, at one accelerator, a maximum equilibrium gas concentration of 5×10^{-4} µCi/cc.[8] This was composed of 45% ^{15}O and 55% ^{13}N. However, similar operating conditions at the second linac produced a concentration of 4×10^{-5} µCi/cc. This difference was attributed to the lack of ventilation at the second facility which limited the amount of air available for interactions with the post-target beam. The authors also observed a strong dependence of gas concentration on the target arrangement, especially local shielding. Lack of such shielding allows more radiation to interact with air, producing higher concentrations of radiogases. Use of an aluminum target in place of tungsten did not significantly affect gas production.

Measurements at a 40 MeV linac, discussed in reference 9, detected trace amounts of ^{39}Cl and ^{41}Ar, as well as the more common air activation products ^{11}C, ^{13}N, and ^{15}O. Production rates of the latter three nuclides ranged from <.1 µCi per pulse of 20 MeV electrons, without a bremsstrahlung target, to 2 µCi per pulse of 45 MeV electrons, with a bremsstrahlung converter. Relative proportions of the nuclides were found to be extremely dependent on the operating energy, since many of the operating energies are near or below one or more of the thresholds of the (γ, n) production reactions. Total facility release quantities were given as being "in the curie range."

The calculation of radioactive gas production rates at a 100 MeV electron linac is the subject of reference 19. Using a theoretical bremsstrahlung energy spectrum

and gamma-neutron cross sections for oxygen and nitrogen, production rates were calculated for ^{13}N and ^{15}O. Equilibrium concentrations of these nuclides were calculated to range from 10 to 1000 μCi/m^3, depending upon room size and ventilation rate. It was pointed out that electron linacs must be capable of energies of 50 MeV or more to activate nitrogen and oxygen via the (γ,n) reactions.

The author also calculated an occupational $(MPC)_a$ of 4 x 10^{-6} μCi/cc based on an external dose due to ^{13}N. It was shown that a wait corresponding to 10 air changes ($\sim$1 hr) is necessary after shutdown before uncontrolled access to the target room can be permitted. Finally, the author mentions that exposure hazards outside the target rooms will be generally insignificant if the exhaust is discharged from a stack extending above the roof of the building.[19]

Reference 10 discusses in great detail the release of gaseous tritium from a Cockcroft-Walton neutron generator. This machine produces neutrons by deuterium bombardment of a tritium/titanium target [T(d,n) reaction]. During irradiation of the targets, which typically contain about 5 curies of tritium, some tritium is sputtered off of the target surface. Although the target is contained in the evacuated beam tube, tritium can be released to the room through the vacuum pump exhaust. The amount released in this manner is esti-mated to be 100 to 300 mCi per target expended. Finally, the authors recommend a simple tritium trapping system for the vacuum pump exhaust.

The remaining articles deal with two main topics: 1) gas and dust activation at high energy (BeV) accelerators, and 2) stray radiation characteristics of smaller (MeV) machines. The high energy accelerators are essentially all excluded from this study due to being Federally controlled or non-U.S. machines. Never-theless, the published information on radiogas formation at these machines will be briefly reviewed.

References 11 through 15 discuss radiogas production at two proton accelerators having maximum energies of 600 and 800 MeV, and two high energy electron linacs.

The predominant gaseous nuclides formed at all machines were ^{15}O, ^{11}C, ^{13}N, and ^{41}Ar. Gas concentrations at the proton accelerators ranged from 2×10^{-5} to 7×10^{-3} $\mu Ci/cc$. Those at the 150 MeV electron linac averaged 1.0×10^{-6} $\mu Ci/cc$ ($^{15}O + ^{13}N$) and 2.4×10^{-7} $\mu Ci/cc$ (^{41}Ar), during beam runs.[15] Investigators at the 550 MeV electron linac were able to detect ^{7}Be, ^{24}Na, and ^{56}Mn produced by dust activation.[14]

From the dosimetry discussions in these references, it was concluded that the skin is the critical organ due to the predominant beta dose,[12] and that this dose contributes only a small fraction of the total annual offsite dose.[10]

Neutron flux around smaller accelerators is the subject of references 16, 17, and 18. Knowing the thermal neutron flux allows calculation of the production rates of those isotopes produced (by n,γ) reactions. A useful value obtained was 440 $n/cm^2/sec$ measured in the treatment room of a Clinac 18 medical accelerator.[17]

5.2 Data from Study Facilities

Two facilities were selected for gaseous effluent monitoring in this study: the 100 MeV isochronous cyclotron at the University of Maryland and the 6 MeV positive ion Van de Graaff located at the University of Kentucky.

Three potential sources of airborne radioactivity were investigated at each facility before beginning the actual sampling. They were the machine cavity, the beam tube vacuum pump(s) exhaust, and target preparation hoods. At the cyclotron, a large, centrally located exhaust duct (see Figure 5-1) carried the cavity exhaust air and the vacuum pumps' exhaust to a roof vent at 481,000 liters/min (17,000 cfm). The air turnover rate in the cavity was estimated to be 6 to 7 air changes per hour. Target preparation hoods were not utilized during the study period.

The Van de Graaff cavity employed a closed air circulation system operating at about 13,000 liters/min (4000 cfm) (return side). The return air was sampled,
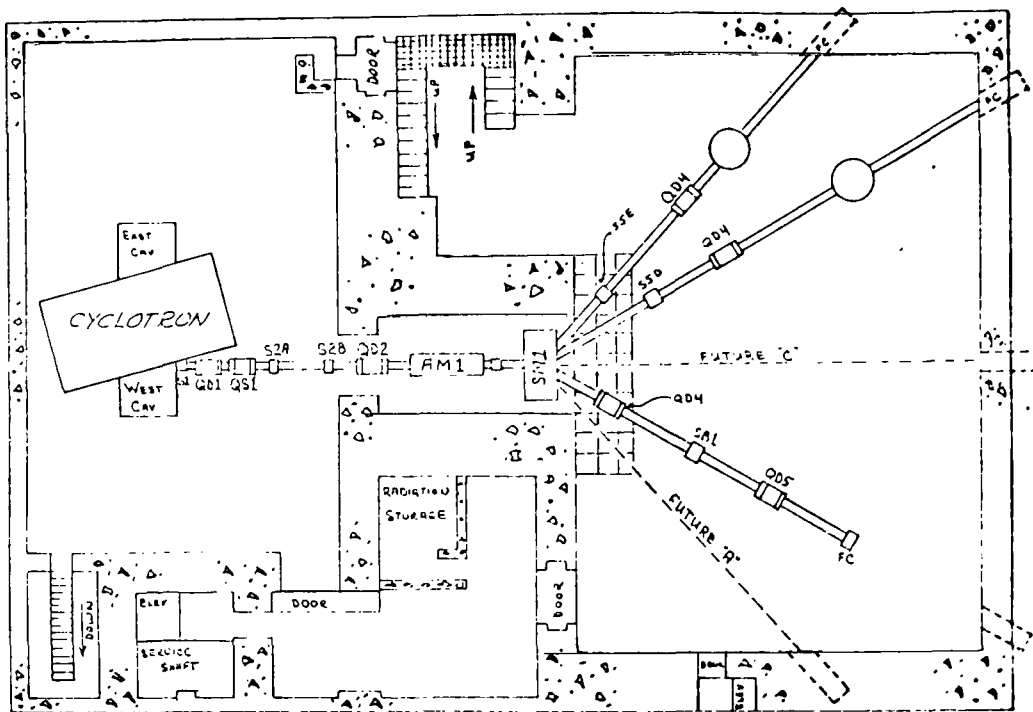
Note: At the center of this top-view schematic is the "magnet shaft." Here the beam is carried vertically, as well as horizontally (as shown), to another level of experiment areas. The single ventilation air exhaust duct is located at the top of the magnet shaft. Thus , the air flows from the cyclotron room and experiment areas into the magnet shaft (through breaks in the shield walls), into the exhaust vent and up to the discharge point on the roof.

FIGURE 5-1

SCHEMATIC OF CYCLOTRON FACILITY

although this air was not released to the atmosphere. The vacuum pumps'
exhaust was piped to the top of the cavity "silo" where it was vented near
a small roof ventilation fan (see Figure 5-2). Finally, a fume hood where
gaseous tritium targets were handled was sampled where it was vented atop
the building. The flow in this vent was measured to be approximately 17,000
liters/min (600 cfm).

No effluent treatment systems were in place or in use on any of the ventila-
tion systems described above.

5.2.1 Sampling Techniques

Sampling was performed by drawing a gaseous sample from the release plenum or
stack and collecting the sample in a chamber or on a trap. The flow rate of
the sample line was about 28 liters/min (1 cfm) through the filter cartridge
and about 7 liters/min (.25 cfm) through the silica gel. The schematic of the
sample train is shown in Figure 5-3. A summary of the sampling equipment used
is presented in Table 5-1.

A specially fabricated 2-liter gas collection chamber was also used. The
chamber was designed to fit over the gamma detector in a Marrinelli flask
configuration. The chamber was evacuated prior to sample collection. Details
of the sampling techniques are given in Appendix B.

5.2.2 Detection Techniques

Three instrumentation systems were used in this study for the detection of radio-
activity in gas and filter samples. For the detection of gamma (and positron)
emitting nuclides, a Ge(Li) spectrometry system was used. A 60 cc lithium
drifted germanium detector was coupled to a 4096 channel pulse height analyzer
(Canberra 8180). Spectra were stored on magnetic tape for later analysis. This
allowed sequential spectra to be taken on the same sample.

Silica gel was used in the sampling train to trap HTO. After sampling, the
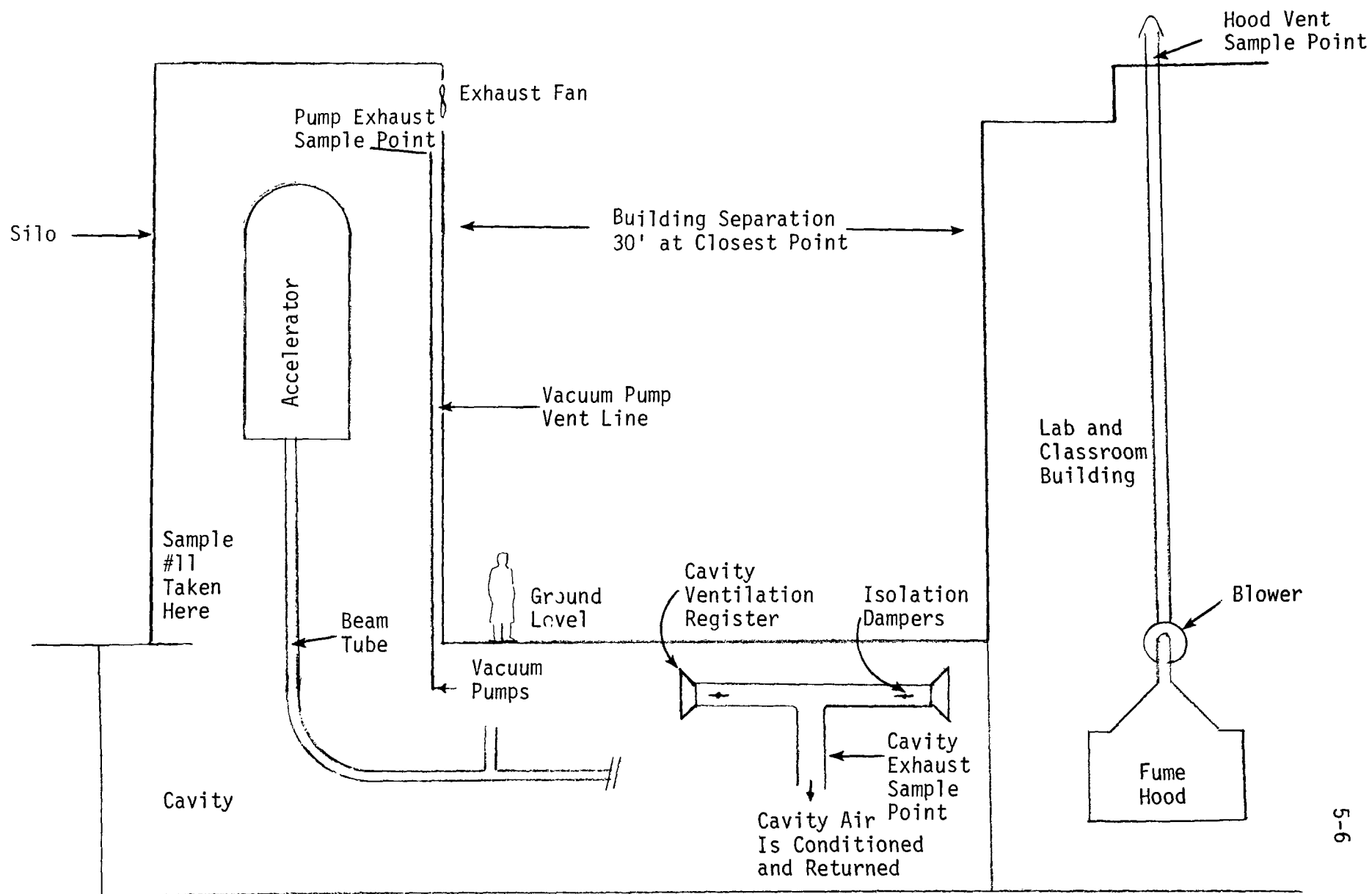
FIGURE 5-2. SCHEMATIC OF VAN DE GRAAFF FACILITY
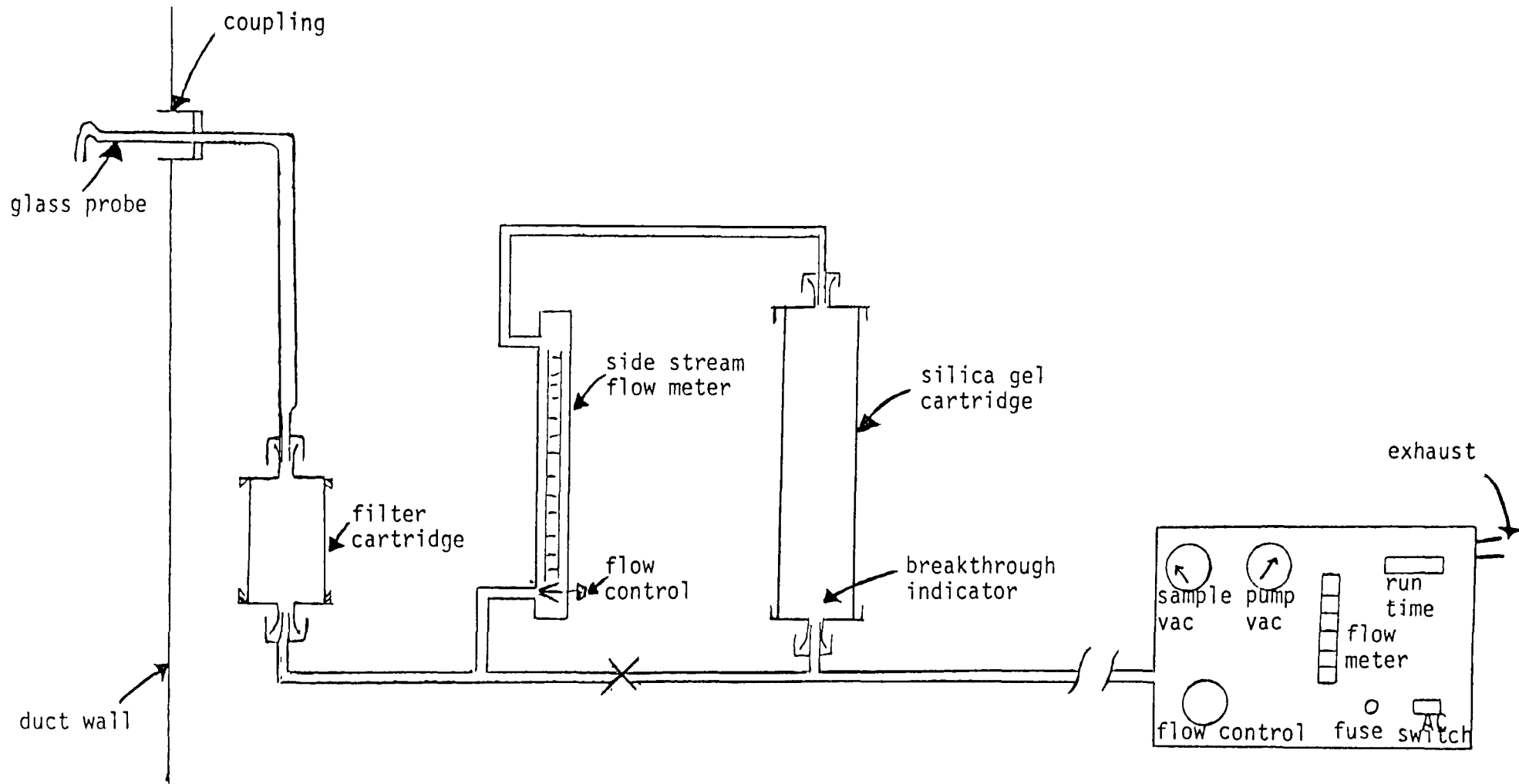
FIGURE 5-3.   SAMPLE TRAIN SCHEMATIC

TABLE 5-1

DUCT SAMPLING EQUIPMENT

FUNCTION	MATERIAL or ITEM
Particulate filter	Glass fiber HEPA
Iodine and gas filter	Activated charcoal
Carbon dioxide filter	Sodium zeolite (NaX)
Water vapor (HTO) filter	Grade 05 silica gel 6-16 mesh
Breakthrough indicator	Grade 42 silica gel 6-16 mesh
Air pump/flow meter	Radeco model HD-28/B

silica gel was weighed, mixed, and a 3-gram sample was added to 4 cc of liquid scintillation solution. The mixture was counted on a Beckman LS-150 liquid scintillation detector discriminated for tritium beta radiation.

Finally, selected CO_2 samples (collected on a molecular sieve) were analyzed for ^{14}C. This was accomplished by driving off the trapped gases with heat, identifying the off-gases with a gas chromatograph, and isolating the CO_2 driven off. The fraction was then counted in a 100 cc gas proportional counter.

5.2.3 Results

The largest amount of radioactivity produced at the cyclotron was detected on February 6. On this date, the machine was delivering 100 MeV protons to a beryllium/aluminium target, ultimately yielding fast neutrons with energies distributed around 100 MeV. Beam current was approximately 2μA at the target.

Nitrogen-13 was detected on the activated charcoal sampler. The physical form is gaseous since particulate activity was not detected. The chemical form of the ^{13}N is still in doubt since many nitrogen compounds (even N_2) can be trapped in activated charcoal. A backup charcoal cartridge also contained ^{13}N (about 17% of the quantity that was detected on the front cartridge). Based on the activities detected on the two cartridges, a collection efficiency of 83% is calculated.* The decay curve of the sample activity is shown in Figure 5-4.

The molecular sieve sampler, as expected, collected carbon-11 dioxide. The results of the February 6 sampling are shown in Figure 5-5. No other runs produced detectable ^{11}C activity. The collection efficiency was determined to be 8% at 28 liters/min. Although ^{15}O was present in the exhaust gas (see below), it did not form $C(^{15}O)_2$ and was not collected in this sampler.

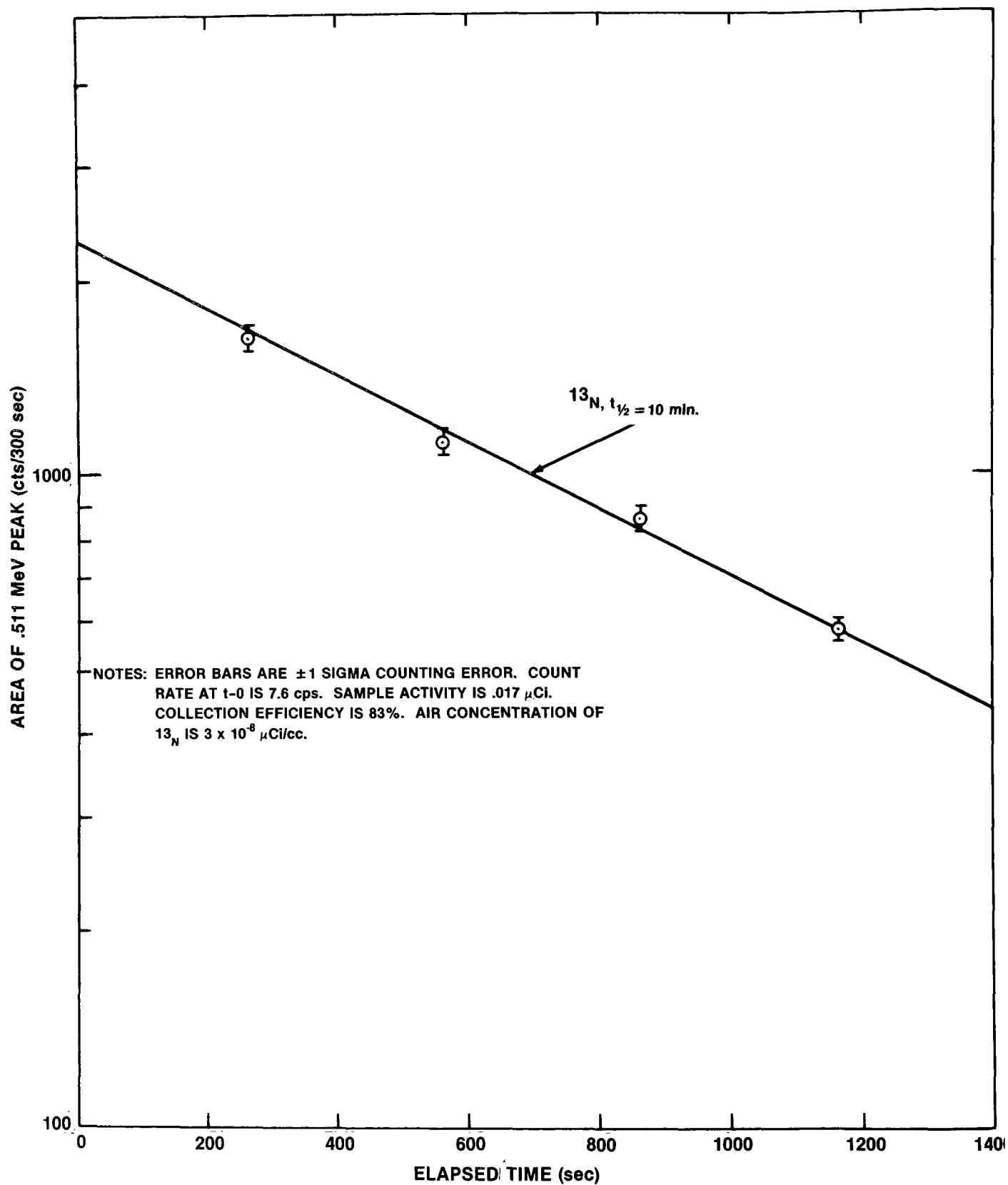---

*Efficiency = $1-(B/A)$

FIGURE 5-4
DECAY OF ACTIVITY ON CHARCOAL-A SAMPLE, FEBRUARY 6
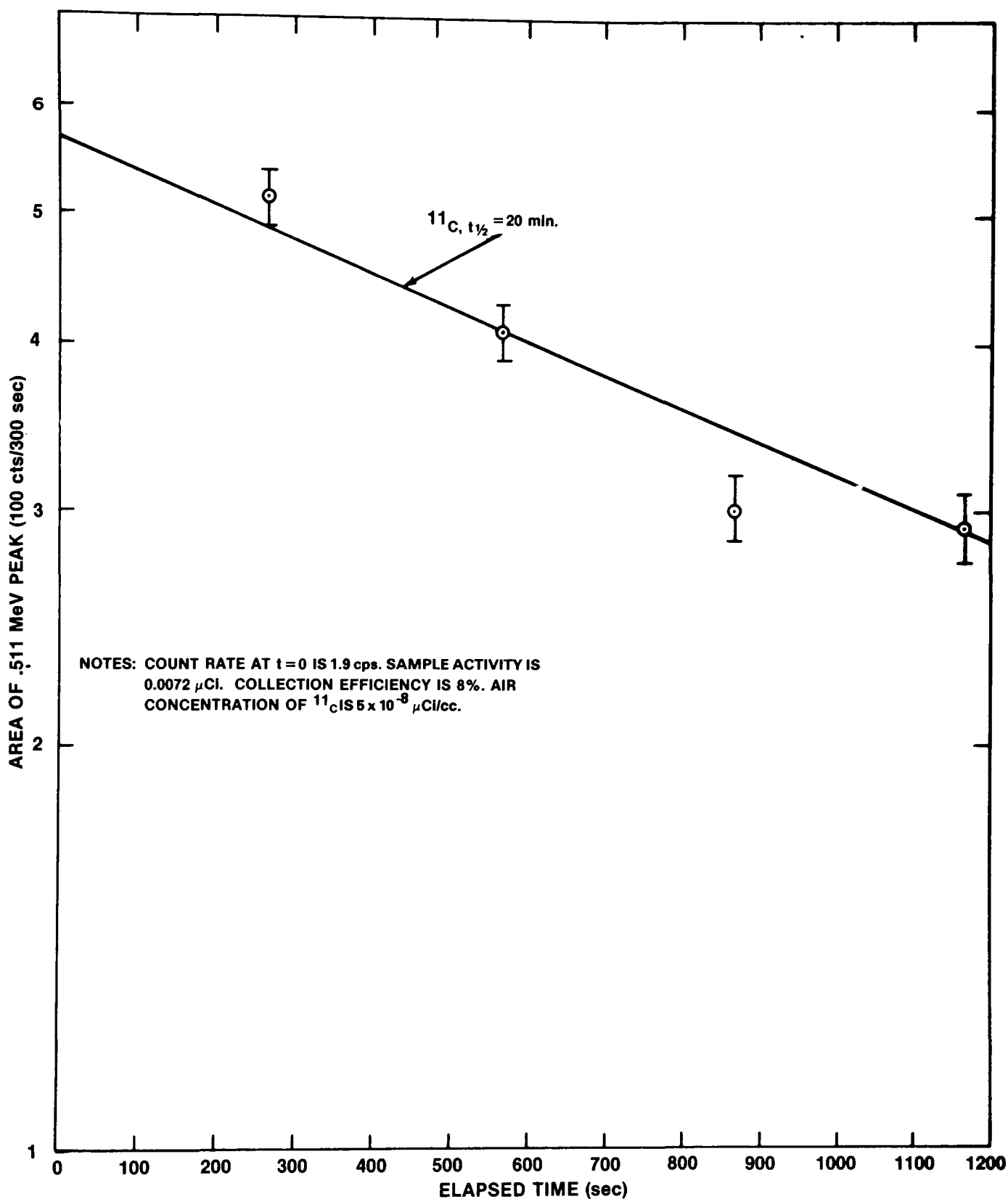
FIGURE 5-5
DECAY OF ACTIVITY ON NaX-A SAMPLE, FEBRUARY 6

One of the two gas samples taken on February 6 contained activity decaying with the two-minute half-life of ^{15}O (see Figure 5-6). The second gas sample, taken with the beam off, showed no residual activity. The concentration of ^{13}N and ^{11}C were too low to be detected in this manner. The relative concentrations of these isotopes agree fairly well with those predicted in Section 4.3; however, ^{13}N was in relatively lower concentrations than predicted.

The only other activity detected at the cyclotron was trace ^{13}N activity on January 27, 30, and 31. The concentrations fluctuated around 10^{-9} μCi/cc. No tritium was detected at this location. Results of the gamma ray and tritium measurements are given in Appendix A.

The measurement at the Van de Graaff accelerator had a different focus. At this location, the positron emitters ^{15}O, ^{13}N, and ^{11}C were not detected, but tritium was found. The source of the tritium was a target assembly containing ~130 curies of tritium on a uranium "getter." The target cell held 1.5 curies and was separated from the beam tube by a molybdenum foil.

Several pathways exist from the gas cell into the ventilation air. In the first, tritium travels into the beam tube through minute holes in the foil. In fact, tritium contamination had been found to exist within the beam tube. Gases in the beam tube would be vented at the top of the cavity by the vacuum pumps. When holes in the foil are detected, the tritium in the gas cell is reabsorbed on the uranium and the target assembly is removed. Some tritium may escape during this operation. Finally, the assembly is carried to a fume hood where the foil is replaced and leak tested with helium. Tritium may also escape during this operation.

As shown in Table A-2, tritium concentrations were highest in the fume hood exhaust (10^{-5} μCi/cc); the next highest concentrations were in the vacuum pump exhaust (10^{-6} μCi/cc). Tritium concentrations in cavity ventilation air ranged from 10^{-8} to 10^{-7} μCi/cc; the highest levels were detected during bombardment of the tritium target.
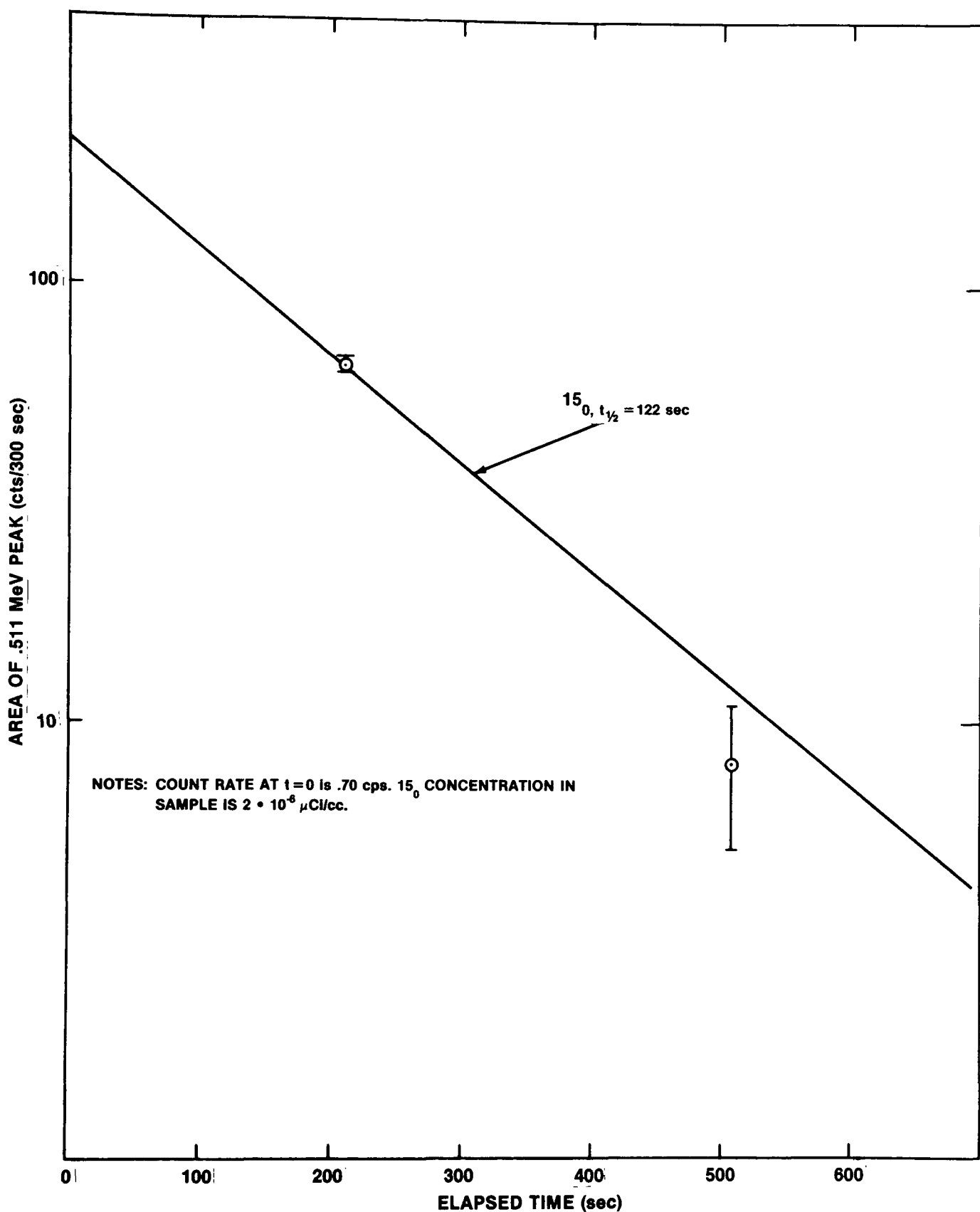
FIGURE 5-6
DECAY OF ACTIVITY OF 2 LITER GAS SAMPLE #1, FEBRUARY 6

Several molecular sieve cartridges from each facility that had collected CO_2 were analyzed for ^{14}C. The results, presented in Table A-3, indicate ^{14}C was present in one of the two samples taken at the Van de Graaff facility and in none of the samples from the cyclotron. Carbon-14 is pro-duced by the $^{14}N(n,p)$ reaction. The thermal neutron cross section is 1.8 barns; that for fast neutrons is about a factor of 10 lower. Using the thermal neutron flux measured in the Van de Graaff cavity (50 $n/cm^2/sec$), a ^{14}C concentration (after 24 hours of operation) of 0.1 pCi/m^3 is calculated. The expected concentration on March 6 would then be 1.1 pCi/m including background; however, 100 pCi/m^3 was measured. This result is even more suspect because it was found in only one of two CO_2 samples that were taken a week apart, under similar neutron beam conditions. The high ^{14}C concentration measured on March 6 remains an anomaly.

5.3 Release Estimates.

As discussed above, operations at the cyclotron involving protons and heavy ions produce small amounts of ^{13}N. Assuming exhaust concentrations of 10^{-9} $\mu Ci/cc$ and a work factor of about 1000 hrs/yr,* approximately 38 mCi/yr are released to the atmosphere. However, when high energy neutrons are produced, ^{15}O, ^{13}N, and ^{11}C are present in the exhaust air from (n,2n) reactions. Release rates for these nuclides are 16 $\mu Ci/sec$, 0.27 $\mu Ci/sec$, and 0.43 $\mu Ci/sec$, respectively. The high energy neutron experiment observed lasted about four hours.

As indicated earlier, two exhaust fans at the Van de Graaff facility actually exhaust to the atmosphere. These are the fume hood exhaust and the small ventilation fan at the top of the cavity (see Figure 5-2). The majority of the cavity exhaust air is recycled. Given the concentration of tritium in the fume hood exhaust, the release rate during foil changing was 0.43 curies per 24 hours. Since the cell capacity during operation is 1.5 curies, this 24-hour release

---

* Determined from facility operating schedules.

constitutes nearly one-third of the tritium used in the cell. However, it is highly unlikely that this quantity of tritium failed to return to the uranium getter during cell evacuation. Either there existed another source of tritium in the hood, or heating of contaminated surfaces occurred releasing tritium, or an equipment failure and/or operational error occurred in the hood. A more definitive description of the source of the 0.43 curies of tritium is not possible without further measurements. Estimating annual releases of tritium from this source is difficult for the same reason. Nevertheless, arbitrarily assuming semiannual releases of this magnitude, the annual release rate would be on the order of 1 curie per year.

The estimated release from the cavity is due to one small (∿23,000 L/min estimated) ventilation fan near the end of the vacuum pump exhaust line. Using the tritium concentration detected 15 meters below the exhaust fan (sample #11), a release rate of 0.022 µCi/sec is calculated. A release rate from the vacuum pump exhaust line was not calculable since flow from this line was too low to be measurable. It is assumed that the above release rate is typical of all accelerator operations using the tritium target; however, this is probably conservative since leakage in the target cell occurred during the study. Using the work factor of the target of 0.36, the annual tritium release from the cavity is estimated at 0.3 curies. Estimates of the tritium inventory on the uranium getter were not available as a function of time.

6.0 EFFLUENT TREATMENT

6.1 Existing Standards for Air Treatment

The existing standards limiting the amount of radioactive gases released to the atmosphere were established in 1961 by the Atomic Energy Commission, under the recommendations of the ICRP and the NCRP. The Maximum Permissible Concentrations in air for radionuclides in unrestricted areas were published in the Code of Federal Regulations Title 10, part 20, and are currently enforceable by the Nuclear Regulatory Commission.[20] However, they apply only to radioactive materials subject to licensing and not to radiation-producing machines such as accelerators.

The Suggested State Regulations for Control of Radiation[21] were initially published in 1962 by the Council of State Governments with the Assistance of the AEC and the BRH. Part D of these model regulations contains standards for protection against radiation based on the 10 CFR 20 limits for unrestricted areas. In 1974, this publication was revised to reflect amendments, new information, and other changes in guidelines, making it compatible with Federal regulations. A section on particle accelerators was added as Part I, "Radiation Safety Requirements for Particle Accelerators." A subsection, Part I.12, "Ventilation Systems," states:

> (a) Adequate ventilation shall be provided in areas where airborne radioactivity may be produced.
>
> (b) A registrant [or licensee], as required by D.106, shall not vent, release or otherwise discharge airborne radioactive material to an uncontrolled area which exceed the limits specified in Part D, Appendix A - Table II, except as authorized pursuant to D.302 or D.106(b). For purposes of this paragraph, concentrations may be averaged over a period not greater than one year. Every reasonable effort should be made to maintain releases of radioactive material to uncontrolled areas, as far below these limits as practicable.

Since the Agreement States have promulgated regulations for their own licensing and/or registration of particle accelerators, it is assumed that the states also follow these suggested requirements for ventilation.

6.2 Treatment Systems

Guidelines for the treatment of air from accelerator facilities are
based mainly on dilution and containment at the source prior to exhaustion.
These ventilation and exhaust procedures and their effect on the concen-
trations of gaseous emissions released to the atmosphere will be dis-
cussed. Air cleaning devices and their cost-effectiveness will be dis-
cussed separately.

6.2.1 Ventilation

Ventilation and exhaust procedures have been recommended by several govern-
mental agencies and private groups with the intent of reducing radiation
levels in the immediate vicinity of the accelerator. The prevailing
philosophy has been that safe levels obtained internally would insure
minimal public exposure.

The American National Standards Institute, with the cooperation of the
National Bureau of Standards, established in 1969 the standard, "Radiological
Safety in the Design and Operation of Particle Accelerators." This
standard requires adequate ventilation of areas where airborne radioactivity
is expected to exceed the Maximum Permissible Concentration* and dispersal
of the vented air in a manner compatible with existing air pollution laws.
Also, precautions should be taken to prevent the possibility of exhaust air
being drawn into neighboring air intakes.[32]

The National Center for Radiological Health under the Department of Health,
Education and Welfare published at about the same time the "Particle
Accelerator Safety Manual." Among its suggested practices for the control
of airborne radioactive materials is the provision of a ventilation system
apart from the building ventilation and so designed that the accelerator
areas are at a lower pressure than the other parts of the building.

---

*10 CFR 20, App. B., Table II.

Additionally, air flow rates should be variable so that air flow can be increased during periods of high beam intensity.[33]

The National Accelerator Safety Committee prepared a similar report for high energy accelerators, but with emphasis on vent system design and maintenance as precautions against the release of hazardous gases in the event of accidental ignition or other equipment failure.[34]

More recently, the National Council on Radiation Protection published "Radiation Protection Guidelines for 0.1-100 MeV Particle Accelerator Facilities." Included in this report is a discussion of ventilation and ducting. Exhausting the air nearest the electron window and the use of high capacity blowers are among the suggestions for the reduction of hazardous gases that accumulate. The necessity for controlling dust and other particulates by filtration is also mentioned.[35]

Ventilation practices vary widely according to the mode of operation of the accelerator and the physical layout of the facility. The proper balance between ventilation of the work area and decay of radiogases must be determined prior to release. A high ventilation rate too quickly after operation would allow the discharge of unpermissible amounts of radioactive gases to the atmosphere. In cases where there are adsorption filters, the reduced residence time would affect their efficiency. While a comfort-index would require a minimum of 2-3 air changes per hour, there is a maximum above which the operational efficiency of sensitive instruments may be affected.

Several papers have been found in the literature regarding induced radioactivity in accelerator operations at beam energies greater than 10 MeV. Some of these references are to non-U.S. or Federally-owned machines and thus outside the scope of this report. Their review here is for instructive purposes, especially when ventilation or exhaust conditions are described.

In the exhaust from the operation of a 20-40 MeV linear accelerator, the ^{15}O and ^{13}N air-activation components were determined to be less than 1% of the Maximum Permissible Concentration* for airborne emissions. The accelerator room was constantly ventilated and exhausted at a rate of 1.1×10^6 L/min (40,000 ft^3/min) from a 20-meter stack.[9] Two other medium energy linac facilities were monitored for the occurrence of ^{15}O and ^{13}N off-site; the concentrations were within the limits for nonoccupational exposure. At one linac, air supply and exhaust configurations are as follows: two fans, operating in parallel, move target and accelerator room air to the base of the 20-meter stack from an exhaust filter bank 3.7 meters off the floor and forward of the target. Air treatment consists of a set of prefilters, followed by a set of HEPA filters. The exhaust flow rate was 378,000 L/min (13,500 ft^3/min) providing 11 air changes per hour which is almost half the design capacity. The author attributed this to dust loading on the filters.

For the other linac described, the target is located in a caveroom, unventilated but exhausted through the roof at ground level at a rate of 70,000 L/min (2,500 ft^3/min) or 6 air changes per hour; leakage from around doors and ports accounts for the make-up air.[8]

A method described by Kase to predict ^{13}N and ^{15}O concentrations in air from a 100 MeV linac is important to mention because it can be applied at the design stage of similar facilities to determine ventilation criteria. For a known beam length, for example, activity concentrations can be calculated for varying room sizes and ventilation rates.[19]

In the operation of a 550 MeV linear accelerator located underground, it was found that concentrations of the radiogases from the stack exceeded the MPC_a, especially during operation. The author recommended confining the target room in a closed air circuit for a decay time and reducing the exhaust volume by 50%.[14]

---

* 10 CFR 20, App. B., Table II.

The operations of the CERN 600 MeV synchrocyclotron and the 28 GeV synchrotron were examined for gaseous emissions prompted by an anticipated 10-fold increase in beam intensity. Modifications of the ventilation system, increased stack height (to 25 meters), and the continued use of high efficiency filters were indicated.[11]

The combined effects of decay and dilution necessary to reduce the concentration of emissions from the stack of a 200 GeV machine tunnel have been reported by Thomas.[22] The activity of the air confined in the tunnel after machine turn-off was calculated to be 360 curies. Assuming a leakage rate of 10% per hour to the stack at a travel time of 6 minutes, Thomas determined that as many as 4 curies per hour would be released to the atmosphere. Since 90% of the total specific activity is found close to the target and drops by a factor of 10 after 10 minutes, the author recommends enclosure of the target area and exhausting after 10 minutes only those areas to which access is required.

Special problems arise with the use of tritium targets for neutron generators. Gaseous tritium (^{3}H), the radioactive isotope of hydrogen, has been detected in the exhaust gas from a Cockcroft-Walton neutron generator used to bombard a tritium target. It can be considered hazardous owing to its long half-life and its low-energy beta radiation. In studies of tritium contamination in particle accelerators, it has been shown that the tritium was readily absorbed in the lucite insulators of the ionization chambers.[10]

Several references mention ozone contamination of air during electron beam operation. According to the American Conference of Governmental Industrial Hygienists, ozone is a highly injurious and lethal gas with a Threshold Limit Value of .1 ppm.[35] One source indicates that hazardous levels of ozone can be produced even at low energies. An example is given for a 1-mA external beam of 10-MeV electrons with a path length of 300 cm which is contained in a unventilated room 4 m by 4 m by 3 m. After an irradiation time of about 15 minutes, the concentration of ozone was 15 ppm. The use of ducts or hoods with air intakes located as near the electron-permeable window as possible and the use of high capacity blowers are recommended.[35] In air

activation studies, Slabak confirmed the predominance of ozone production in the 13 to 20 MeV range. Also, it was determined that the decomposition rate of ozone is sufficiently long that its disappearance is governed primarily by ventilation.[9] The effects of ventilation on radiogas and ozone concentrations from 40 to 50 MeV linacs were studied in detail by George and his coworkers, who found initial concentrations of ozone up to .8 ppm after beam-off. With ventilation, reduction by a factor of 10 was possible after 15 to 20 minutes. In the absence of ventilation, the reduction was only half over a period of 35 minutes. The use of a local exhaust system (moveable hoods) that could be adapted to the target configurations was suggested in this report.[8]

6.2.2 Air Cleaning Devices

The air cleaning technology that exists for conventional processes can be adapted to the treatment of gaseous effluents from accelerators with a few basic exceptions:

1. The lowest threshold limit for chemical pollutants is two orders of magnitude higher than the MPC of any radioactive gas.

2. Airborne particulates, which are irradiated by adsorption of or association with radioactive gases, are generally in the submicron range. Also, the dust loading or amount of particulate matter in accelerator exhaust is low due to the comparatively clean conditions of these facilities. These factors would limit the selection of filters to those with a high removal efficiency for submicron particles.

Another departure from conventional processes is that the function of adsorptive filters is simply to trap the gases for a decay-time; recovery or regenerative techniques are of no interest. In fact, the replacement of spent filters might present special problems if there is residual long-lived activity on the filters.

The Nuclear Air Cleaning Handbook, published by ERDA in 1976, is considered a reliable guide for the design and installation of high efficiency air cleaning systems for the nuclear power industry with some attention given to radiochemical operations.[23] Extensive research in this area has also been the subject of biannual Air Cleaning Conferences, the latest of which was held in August 1978.

In the absence of an authoritative guide specific to accelerators, these sources can be useful in establishing the principal features of the mechanical or hardware phase of an air cleaning system, but wide differences limit their applicability. For example, accelerator users are primarily institutions (hospitals, universities, processing plants) with only a portion of their facilities restricted for these activities. In some cases, existing ventilation and air conditioning configurations have to be modified to accommodate the air flow to and from the accelerator room. The volume of air to be treated and the concentration of contaminants are usually less than that of most nuclear processing systems. Elaborate methods of trapping iodine and krypton gases are not of primary concern and rigorous provisions for high temperatures, moisture, and other emergency conditions are not necessarily applicable.

The principal control methods for radioactive effluents can be discussed as two distinct types, employed singly or in combination. The first type consists of the ventilation controls that direct the contaminated air into an exhaust system to a controlled release point. The second type of controls remove contaminants from the exhaust stream prior to release either permanently, in the case of particulates, or temporarily to permit decay to safe levels.

Pressure Zonation

This ventilation principle consists of providing sufficient pressure differentials between the zoned-area and the rest of the building so that there is no backflow of contaminated air to spaces of uncontaminated air. Examples of

this are hoods, wall fans, and vent stacks. The airflow induced by hoods and wall fans permit dilution of radioactive effluents within the occupied area of the facility, but the vent stack provides the most rapid dispersion of effluents due to its elevated release point and high effluent velocity.

Filtration

The filtration of exhaust air prior to release is usually accomplished by HEPA filters, preceded by pre-filters. In some cases, adsorptive filters are necessary for the removal of gases. Examples of these are activated charcoal and molecular sieves, but these are usually preceded in line by a particulate filter.

HEPA filters, described as dry-type extended medium filters, consist of pleated webs of fiber glass papers. Their particle removal efficiency is 99.97% for .3 micron particles. The most frequently used HEPA filter is rectangular and is designed for a nominal airflow of 28,000 L/min. For larger air volumes in central systems, the filters can be arranged in banks or in multiple single-units in series. Above 8.5×10^5 L/min the bank systems are segmented into parallel systems. Self-enclosed single-stage filters, or caissons, for in-duct installation are commercially available. One type is designed with a bag-out feature, permitting the replacement of filters with minimum personnel exposure.

Roughing filters are required in advance of the HEPA filters to protect them from larger particulates. The extended-medium dry-type units that have replaceable mediums or consist of throw-away cartridges are desirable.

Adsorptive filters of activated carbon are used to trap hazardous gases and their reaction products from the air stream. Most commonly used are modular tray adsorbers, which are arranged in banks for multi-stage air cleaning. Their dimensions correspond to standardized openings and contain around 23 kg of carbon in two 5-cm beds separated by an air space.

Each tray is designed for a gas residence time of .25 sec and an air flow rate of 9424 L/min. Replacement of these filters is usually necessary once a year. Also available are "caisson" housings, with the bag-out filter changing feature. They can be used singly or arranged in groups within a single housing. They are designed to accommodate not only the carbon filters described above, but also standard pre-filters and HEPA filters.

In the case of tritium contamination of air, a more elaborate system of air cleaning is necessary. Tritium exhaust systems described for neutron generation consist of a preheater, a catalytic recombiner, and a regenerable molecular sieve bed. Although these components are commercially available, one manufacturer was found to market a packaged adsorption unit, complete with mechanical filters for dust removal. The desirable feature of this device, it is claimed, is that the service life of the filters is unaffected by high concentrations of tritium.[27]

Pretreatment of Ventilated Air

A major portion of dust and particulate matter collected by filters actually consists of atmospheric dust introduced by supply air, or "infiltration," as opposed to internally-generated particulates. Installation of fiber filters on the inlet side of ventilation air would reduce the irradiation of ambient dust particles. Treatment of ducts to minimize corrosion and flaking is another measure that could be taken.

6.3 Costs and Effectiveness

The cost of air cleaning systems varies according to the size of the facility, the ease of installation , and the degree of purification desired. The initial expenditures include the following plus the cost of labor for each:

- The major control equipment (hoods, filters, housings, mounting frames, etc.)

- Ancillary components (fans, blowers, duct work, electrical connections, etc.)

Operating costs will vary with the volume of air, the pressure drop, operating time, and power use by fans, motors and pumps. Maintenance costs will consist mainly of the labor associated with filter replacement, inspection and repairs, in addition to the costs of filters. For example, the pressure drop obtained with prefilters of increasing efficiency will affect the costs of power, installation and replacement, and should be balanced against the costs related to frequency of HEPA filter exchange.

A wide variety of complete systems and components is readily available from vendors. Table 6-1 shows cost estimates for air treatment systems and components based on information obtained by Teknekron from various sources. Except where noted, these estimates were based on a nominal airflow of 28,300 L/min, which is the standard sizing of most air filtration equipment. These figures also represent modifications to existing ventilation systems, so that the wide ranges in estimates are accounted for by varying site-specific installation factors. For comparison, several cost figrues were obtained from the literature for building ventilation exhaust air cleaning systems in the nuclear industry.

Installation figures include the price of ancillary components, such as duct work, blowers, wiring, and associated labor costs. The annual operating costs for HEPA and HEPA/Activated carbon systems include the replacement costs of the filters. The activated carbon filters are usually replaced once a year at a cost of about $330 per 28,300 L/min for an unimpregnated nuclear grade carbon.[36] Replacement frequency for HEPA filters is partially determined by the dust-holding capacity, and for design purposes is considered to be 1809 g for the standard-sized unit.

In the tritium clean-up system, described in reference 36, the annual operating cost includes the processing and shipment off-site of the spent molecular sieve beds.

TABLE 6-1

COST OF AIR TREATMENT CONTROLS (1978 DOLLARS)

SYSTEM	EQUIPMENT	INSTALLATION	ANNUAL OPERATING AND MAINTENANCE
Wall Fan	$300 - $1000	+	$30 - $300
Hood	2000 - 4000	$6,000 - $20,000	+
Vent Stack (2-3M)	10,000 - 60,000	+	+
HEPA Filter	150	3,000 - 10,000 *(4,900 - 14,160)	300 - 500
Prefilter	75		
Housing, etc.	1500		
Vent Stack/HEPA	3,500 - 10,000	10,000 - 60,000	+
HEPA/Activated Carbon	6,000 - 12,000 **(9,700)	+	700 - 1400 **(1200)
Tritium Absorption (56.6 L/min.)	***121,000	+	***(36,300)
Nukem Tritium Absorber (200 L/hr holding tanks)	120,000	120,000	+

*Source, Reference 23, p. 251. 1978 dollars obtained by multiplying 1975 costs by 1.211 based on the Consumer Price Index Listing.

**Source, Reference 25, 1978 dollars obtained by multiplying 1975 dollars by 1.211 as above.

***Source, Reference 36.

+Variable and/or not available

In summary, the existing control technology for radioactive effluents consists of any one or combinations of the following: confinement, dilution, and removal of contaminants by filtration. Costs vary widely according to the air flow to be treated, the desired efficiency, and the modifications entailed for existing ventilation systems.

7.0 GENERIC FACILITIES

In this section, the information obtained is generalized to the various classes of accelerators (constant field, incremental acceleration, and magnetic field). It is recognized that machines can vary greatly within a given class. For instance, a high energy research cyclotron is very different from a high current, isotope production cyclotron. Nevertheless, some generalizations can be made.

7.1 Characteristics

Within the constant potential classification, Van de Graaff accelerators are the most prevalent. As shown in Section 3.2, about 18% of all registered machines in 1977 belonged in this category. Furthermore, 78% of the Van de Graaffs were in the energy range of 1 to 19 MeV. This suggests an intensity ranging from 1 µA to 1 mA (see Figure 7-1). Therefore, the Van de Graaff monitored in this study and discussed in Section 5.2 (6 MeV, 1 to 10 µA) can be considered a generic constant field machine.

The most popular accelerator currently in use belongs in the second class, incremental acceleration or cyclic machines.   This accelerator, the linac, represents about half of the accelerators in the United States. About 90% of these are electron linacs in the energy range of 1 to 19 MeV and are between 1 and 10 kilowatts in power. These characteristics are typical of the cancer therapy machines widely used in U.S. hospitals. For this reason, we have selected an 18 MeV medical linac as a generic cyclic machine.

As discussed in Section 2.0, the betatron machine is in a class of its own. However, its radiation characteristics and even its applications are similar to the electron linac described above. The calculated production of airborne radioactivity by the generic linac can also be applied to the betatron,
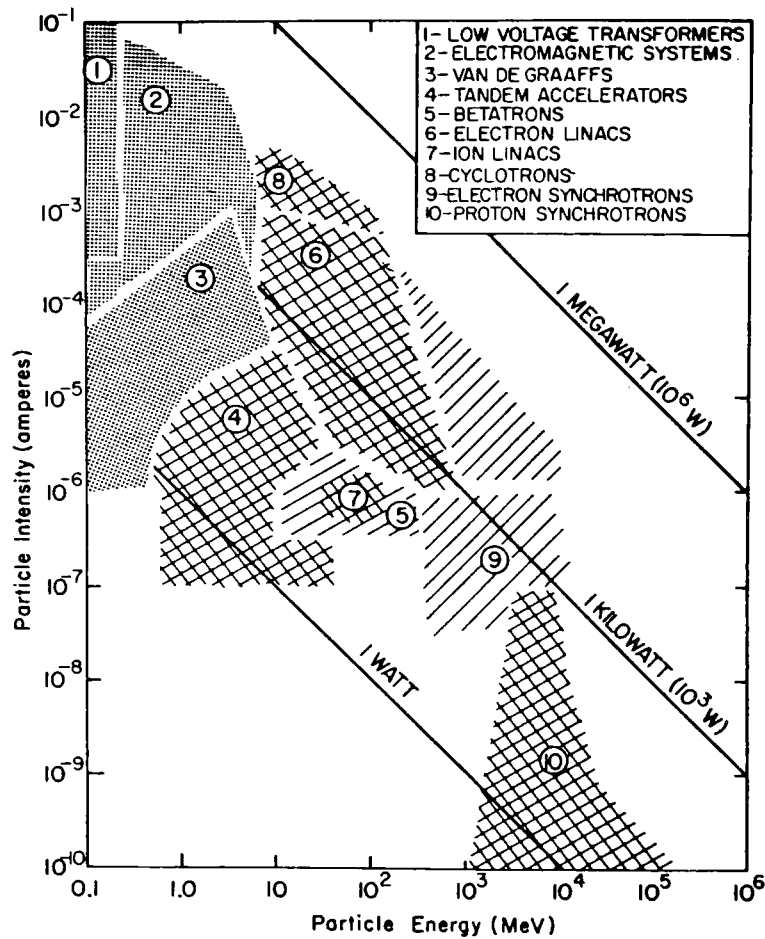
FIGURE 7-1

Particle-beam intensity versus particle energy, for several types of accelerators. (Dark-toned areas relate to accelerators both electrons and ions; middle tones relate to ion accelerators only; light tones relate to electron accelerators only.)

and therefore the magnetic field machine will not be discussed generically. Instead, we have chosen to discuss another cyclic machine, the cyclotron. Our survey shows that these machines are generally higher in energy and higher in power than other machines in use, thus potentially producing greater quantities of airborne radioactivity.

7.2 Release Estimates

The following release estimates for the generic facilities are developed from the field studies described in Section 5 and from calculations discussed in Section 4.

7.2.1 Constant Field Accelerator

The generic constant field machine delivers a beam in the energy range of 1 to 19 MeV, which is, for the most part, below the threshold energies for air activation shown in Table 4-1. The machine produces a small thermal neutron flux,* but this flux is not large enough to produce a measurable amount of activation product.

The field study has shown, however, that measurable quantities of tritium can be released from a facility using a gaseous tritium target. The literature indicates that this is also true of facilities using solid tritium/titanium targets. Our data show that an annual release on the order of 1 curie of tritium is possible due to target maintenance work. Releases due to tritium escaping from the target and beam tube are dependent on the facility design and operation but can be as high as several curies annually. Therefore, the annual release of tritium from the generic Van de Graaff is estimated at about 1 curie. There are about 100 ion Van de Graaff machines in the United States.

*The thermal neutron flux at the study Van de Graaff was measured to be about 50 n/cm^2/sec.

7.2.2 Electron Linac

This machine was selected because of its frequent use in medicine. The great majority of linacs fall into the energy range from 1 to 19 MeV. However, machines of this energy are not capable of producing significant airborne radioactivity for the reasons discussed immediately above. Nevertheless, cal- · culations were made of ^{41}Ar and ^{14}C production rates based on available data. Given the thermal neutron flux around an 18 MeV linac obtained from the litera- ture, annual releases of 100 μCi ^{41}Ar and 10^{-3} μCi ^{14}C were estimated. There are about 440 such linacs in the United States.

7.2.3 Cyclotron

The release estimates for a generic cyclotron apply to a high energy, low current machine, such as the one monitored as part of this study (see Section 5.2). The acceleration of ions at about 100 MeV into scattering targets produced secondary radiation in the form of hard gamma rays (>10 MeV). These gammas were presumably responsible for producing the ^{13}N (via the (γ,n) reaction) detected in our study. The absence of ^{15}O and ^{11}C indicates that the gamma fluxes probably dropped off markedly at the higher energies necessary to produce these nuclides. This, in turn, suggests that lower energy cyclotrons would probably fail to produce even ^{13}N.

In the case of neutron beam production at a cyclotron, relatively large amounts of ^{15}O, ^{13}N, and ^{11}C are produced via the (n,2n) reaction. During the 4-hour run with 100 MeV neutrons observed in our study, 0.23 Ci ^{15}O, 342 μCi ^{13}N, and 457 μCi ^{11}C were released to the atmosphere. It is difficult to estimate the annual utilization of a cyclotron for neutron generation except to say that increased research is being performed in this area for medical applications. Assuming, say, 20 hours of neutron beam time, and adding 38 mCi ^{13}N produced as described in Section 5.3, the following annual releases are calculated: 1 Ci ^{15}O, 40 mCi ^{13}N, and 2 mCi ^{11}C. There are approximately 12 such machines in the United States.

7.3 Dispersion Estimates

Gaseous effluents from a vent or a stack undergo dispersion in ambient air upon release. Estimates of effluent dispersion for a typical accelerator facility were made based on annual average conditions by use of the following expression:[29]

$$C(x,\Theta) = \frac{2.5\ Q\ f(\Theta)}{u(h^2 + xR_z(x))}$$

where: $C(x,\Theta)$ = Effluent concentration downwind of the facility (Ci/m^3)

  Q = Emission rate (Ci/sec)

  u = Average wind speed (m/sec)

  h = Building height (m)

  x = Downwind distance (m)

  R_2 = Plume vertical half width (m)

  $f(\Theta)$ = Frequency of the wind toward one of the 16 directional sectors, Θ

The normalized concentrations (C/Q) in sec/m^3 calculated for a typical facility are presented in Table 7-1. The average wind speed for this site is 5.6 m/sec and the building height is 16.8 m.* The calculations also assume the climatic condition of D-stability since this condition, which occurs roughly half the time, is associated with the building downwash effect. For this reason, the calculated annual concentrations represent conservative estimates.

To estimate dispersion of short-term effluent releases, the building downwash effect must be analysed. Plume downwash into the building wake will occur if the height of the release point above the ground is less than 1.5 times the height of the building. Since this is the condition found at most accelerator facilities, plume downwash can be expected to occur. Furthermore, the highest concentrations of released radioisotopes are predicted to occur in the building wake due to the downwash effect. A conservative estimate of the ground level

---

*These values correspond to the actual values associated with the cyclotron facility discussed in Section 5.2.

effluent concentration within the wake is given by the following expression:[29]

$$C = \frac{1.5Q}{uh^2}$$

At greater distances downwind of the facility, the emissions may be treated as coming from a ground level source with an initial plume cross sectional area of h^2:

$$C(x) = \frac{Q}{u(h^2 + 2R_yR_z)}$$

The half widths R_y, R_z are equal to $\sqrt{\pi/2}$ times the more conventional horizontal and vertical dispersion coefficients σ_y and σ_z. The normalized concentrations, Cu/Q, out to 5 kilometers are given in Table 7-2 for the typical facility described earlier. These concentrations represent averaging times in the range of 30 minutes to 1 hour.

7.4 Demography

The survey of accelerators (see Section 3.4) revealed that 76% were located in urban areas. We have selected three actual accelerator facilities located in urban areas as a basis for developing the demography for the generic facility. Two of the facilities were monitored in this study; the third is an isotope-producing accelerator facility located in an urban area.

Demographic data for the generic facility are based on an average of the 1970 census data for the facilities discussed above. The distances for the population count are measured from the facility. The AREA POP computer code at the U.S. EPA, Office of Radiation Programs (Las Vegas Facility), was run to obtain the population distribution. The number of people within the annular rings of 0-1 km, 1-2 km, 2-3 km, 3-4 km, and 4-5 km has been computed for each of the three facilities and then averaged to obtain the population distribution for the generic facility.

TABLE 7-1 NORMALIZED CONCENTRATIONS, C/Q (sec/m^3)
DOWNWIND OF AN ACCELERATOR FACILITY

Distance Downwind (km)

SECTOR	0	1	2	3	4.	5
N	9.9×10^{-5}	6.2×10^{-7}	2.0×10^{-7}	1.1×10^{-7}	7.1×10^{-8}	4.8×10^{-8}
NNE	9.1×10^{-5}	5.7×10^{-7}	1.8×10^{-7}	9.7×10^{-8}	6.3×10^{-8}	4.3×10^{-8}
NE	9.8×10^{-5}	6.1×10^{-7}	2.0×10^{-7}	1.0×10^{-7}	6.5×10^{-8}	4.4×10^{-8}
ENE	8.6×10^{-5}	5.4×10^{-7}	1.7×10^{-7}	9.1×10^{-8}	5.9×10^{-8}	4.0×10^{-8}
E	1.4×10^{-4}	9.0×10^{-7}	2.9×10^{-7}	1.5×10^{-7}	9.7×10^{-8}	6.6×10^{-8}
ESE	2.1×10^{-4}	1.3×10^{-6}	4.3×10^{-7}	2.2×10^{-7}	1.4×10^{-7}	9.5×10^{-8}
SE	1.6×10^{-4}	1.0×10^{-6}	3.2×10^{-7}	1.7×10^{-7}	1.1×10^{-7}	7.5×10^{-8}
SSE	8.6×10^{-5}	5.4×10^{-7}	1.7×10^{-7}	9.1×10^{-8}	5.9×10^{-8}	4.0×10^{-8}
S	7.4×10^{-5}	4.6×10^{-7}	1.5×10^{-7}	7.9×10^{-8}	5.1×10^{-8}	3.5×10^{-8}
SSW	5.6×10^{-5}	3.5×10^{-7}	1.1×10^{-7}	6.0×10^{-8}	3.9×10^{-8}	2.7×10^{-8}
SW	9.9×10^{-5}	6.2×10^{-7}	2.0×10^{-7}	1.1×10^{-7}	7.1×10^{-8}	4.8×10^{-8}
WSW	1.1×10^{-4}	7.0×10^{-7}	3.0×10^{-7}	1.2×10^{-7}	7.8×10^{-8}	5.4×10^{-8}
W	8.8×10^{-5}	5.5×10^{-7}	1.7×10^{-7}	9.2×10^{-8}	6.0×10^{-8}	4.0×10^{-8}
WNW	4.6×10^{-5}	2.9×10^{-7}	9.3×10^{-7}	4.9×10^{-8}	3.2×10^{-8}	2.2×10^{-8}
NW	7.0×10^{-5}	4.4×10^{-7}	1.4×10^{-7}	7.4×10^{-8}	4.8×10^{-8}	3.3×10^{-8}
NNW	7.5×10^{-5}	4.7×10^{-7}	1.5×10^{-7}	8.0×10^{-8}	5.2×10^{-8}	3.6×10^{-8}

TABLE 7-2 NORMALIZED CONCENTRATION AS A FUNCTION OF DISTANCE
FOR SHORT TERM RELEASES

SITE	NORMALIZED CONCENTRATION, $\frac{Cu}{Q}$ (m^{-2})					
	0 km	1 km	2 km	3 km	4 km	5 km
Accelerator Facility	5.3×10^{-3}	1.1×10^{-4}	3.8×10^{-5}	2.1×10^{-5}	1.4×10^{-5}	1.0×10^{-5}

The AREA POP code provided data on the number of census enumeration districts (CEDS) that were searched to obtain the population distribution at selected radii from a point of interest. The CEDS are used as a measure of the population density and expected accuracy of the data. CEDS of at least 6 are needed to assure good confidence in the accuracy of the population data. The data presented in Figure 7-2 are based on CEDS that range from 5 to 104.

Although the generic machine is in an urban area, it is located on a university campus which is not a high-density location. Typically, it would be adjacent to offices, and the nearest residence (or dormitory) would be at least a kilometer away. Land use would be nonagricultural within the city limits, and partly agricultural and partly residential beyond that point.
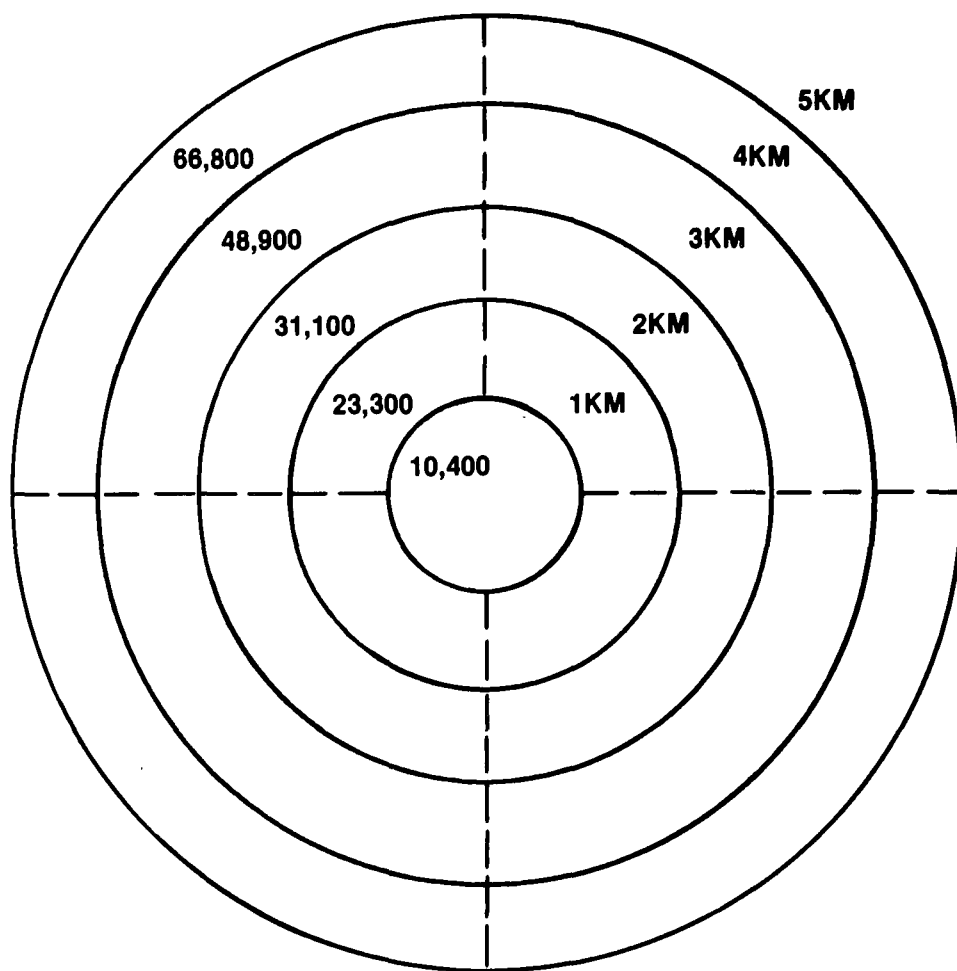
FIGURE 7-2
POPULATION DISTRIBUTION AROUND A GENERIC ACCELERATOR FACILITY

8.0 CONCLUSIONS

The following conclusions have been drawn from the results of this study:

1. Approximately 1200 accelerators were in operation in the United States in 1977 excluding those under Federal control. The growth rate of accelerator use is put at 65 machines per year.

2. The linear accelerator (linac) is the most commonly used machine in the United States. More than half of the machines in use are linacs, and 70% of these linacs are used in medical applications (i.e., cancer therapy) with energies ranging from 1 to 19 MeV.

3. With respect to airborne effluents, machines operating at less than 100 MeV and electron linacs operating at less than 50 MeV produce negligible amounts of airborne radioactivity. Machines operating above these energies produce sufficiently large fluxes of hard gamma rays to produce ^{15}O, ^{13}N, and ^{11}C by the (γ,n) reaction. The exceptions to this are machines used to produce fast neutron fluxes (above 20 MeV) which create the above nuclides by the $(n,2n)$ reaction.

4. The annual quantities of ^{15}O, ^{13}N, and ^{11}C released to the atmosphere by a typical 100 MeV cyclotron are estimated to be 1 Ci, 40 mCi, and 2 mCi, respectively. There are approximately 12 such machines in the United States.

5. Releases of airborne tritium were found at an accelerator facility utilizing gaseous tritium targets for neutron production. Annual release of tritium from a typical facility of this type is put at about 1 Ci.

6. The control of airborne radioactivity around accelerators has two objectives. One objective is to minimize exposure to personnel working in the accelerator cavity. The second is to minimize releases of radioactivity

to the atmosphere. These are somewhat in conflict since high ventilation rates benefit workers desiring quick access to the machine after shutdown but tend to increase the activity released to the atmosphere. To achieve both of these objectives, the following actions are possible:

a. delay discharge of cavity air (and access to the machine) for a sufficient time after shutdown to allow radioactivity to decay to innocuous levels,

b. use recycle type air handling systems with isolation capability for hold-up and for accident situations, and/or

c. use air cleaning systems for effluents or recycled air based on cost/benefit considerations.

9.0 REFERENCES

1. U.S. Bureau of Radiological Health. Report of State and Local Radiological Health Programs Fiscal Year 1977. HEW Pub. No. 78-8034.

2. U.S. Bureau of Radiological Health. The Use of Electron Linear Accelerators in Medical Radiation Therapy, Overview Report No. 2. Market and Use Characteristics: Current Status and Future Terms, 1975.

3. Personal communication with Mr. Tom McRae, Varian Corporation, Extron Division.

3a. Cohen, S.C., et al. Evaluation of Occupational Hazards from Industrial Radiation: A Survey of Selected States, U.S. Department of Health Education and Welfare, Publication No. (NIOSH) 77-142, December 1976.

4. Grey, D.E. (ed.). American Institute of Physics Handbook. McGraw Hill, 1957.

5. Grey, D.E. (ed.). American Institute of Physics Handbook. McGraw Hill, 1963.

6. Patterson, H.W., and R.H. Thomas. Accelerator Health Physics. New York: Academic Press, 1973.

7. Barbier, M. Induced Radioactivity. New York: John Wiley and Sons, Inc., 1969.

8. George, A.C., et al. "Evaluation of the Hazard from Radioactive Gas and Ozone at Linear Electron Accelerators." Proc. U.S. AEC 1st Symp. Accelerator Radiation Dosimetry and Experience (CONF-6511), 1965.

9. Slaback, Lester A. "Health Physics Aspects of 20- to 40-MeV Linac Operations." Armed Forces Radiobiological Research Institute, Bethesda, Maryland (to be published).

10. Nellis, Donald O., et al. Tritium Contamination in Particle Accelerator Operation (NTIS PB-189-362), November 1967.

11. Peetermans, A., and J. Baarli. "Radioactive Gas and Aerosol Production by the CERN High-Energy Accelerators and Evaluation of Their Influence on Environmental Problems." Proceedings of the Environmental Surveillance around Nuclear Installations Symposium, Warsaw, Poland, Nov. 5-9, 1973 (IAEA-SM-180/10), p. 433.

12. Hoefert, M. "Radiation Hazard of Induced Activity as Produced by High-Energy Accelerators." Proceedings of the International Conference on Accelerator Dosimetry Experiments, 2nd 111-20, 1970.

13. Engelke, M.J., and H.I. Israel. "Monitor for Radioactive Gas in the LAMPF (Los Alamos Meson Physics Facility) Accelerator Beam Channel" (LA-5351-MS). Los Alamos, New Mexico: Los Alamos Scientific Laboratory, 1973.

14. Vialettes, H. "Gas and Dust Activation in the Target Room of the Saclay Electron Linac; Identification of the Produced Radioactive Nuclei and Determination of the Rejected Activities." *Proceedings of the International Conference on Accelerator Dosimetry Experiments*, 2nd 121-38, 1970.

15. National Bureau of Standards. *Annual Report - 1975, Health Physics Section*. Office of the Associate Director for Administration.

16. McGinley, P.H., et al. "Dose Levels Due to Neutrons in the Vicinity of High-Energy Medical Accelerators." *Medical Physics*, Vol. 3, No. 6, Nov/Dec 1976.

17. Deye, J.A., and F.C. Young. "Neutron Production from a 10 MeV Medical Linac." *Physics Medical Biology*, Vol. 22, No. 1, 1977, p. 90.

18. Lane, Richard G., et al. "Leakage Radiation Characteristics of an 18 MeV Clinical Linear Accelerator." *Health Physics*, Vol. 35, 1978, p. 485.

19. Kase, K.R. "Radioactive Gas Production at a 100 MeV Electron Linac Facility." *Health Physics*, Vol. 13, 1967, p. 869.

20. U.S. Atomic Energy Commission. *Standards for Protection Against Radiation* (10 CFR 20), 1965.

21. Conference of Radiation Control Program Directors, U.S. Atomic Energy Commission and U.S. Department of Health, Education and Welfare. *Suggested State Regulations for Control of Radiation*, 1974.

22. Thomas, R.H. "Rough Estimates of Radiation Hazard from Radioactive Gas in a Machine Tunnel." Lawrence Radiation Laboratory, Internal Report 10136, 1964.

23. Burchstead, C.A., A.B. Fuller, J.E. Kahn. *Nuclear Air Cleaning Handbook* (ERDA 76-21). Oak Ridge National Laboratory, 1976.

24. U.S. Nuclear Regulatory Commission. *Proceedings of the Fifteenth Air Cleaning Conference*, Boston, Mass., August 1978.

25. U.S. Nuclear Regulatory Commission. *Guide 1.110: Cost Benefit Analysis for Radwaste Systems for Light-Water-Cooled Nuclear Power Reactors*. March 1976.

26. Barnebey, Cheney. "Activated Carbon, Purification and Recovery Treatment" (trade literature).

27. Nukem, Gmbh. "Tritium Technology," N-753-4.1 (trade literature).

28. Eicholz, G.G. (ed.) *Radioisotope Engineering*. New York: Marcel Dekker, Inc., 1972.

30. Silvester, D.J., "Accelerator Production of Medically Useful Radio-nuclides," 1AEA-SM-171/6, 1974.

31. Myers, W.G., et al. "^{123}I for Applications in Diagnosis," 1AEA-SM-171/34, 1974.

32. National Bureau of Standards. Radiological Safety in the Design and Operation of Particle Accelerators. NBS Standard 107, 1969.

33. Brobeck, W.M. and Associates. Particle Accelerator Safety Manual. U.S. Department of Health, Education and Welfare, MORPH68-12, October 1968.

34. U.S. Atomic Energy Commission. Safety Guidelines for High Energy Accelerators, 1967.

35. National Council on Radiation Protection. Radiation Protection Guidelines for 1-100 MeV Particle Accelerator Facilities. NCRP Report No. 51, 1977.

36. U.S. Energy Research and Development Administration. Environmental Statement, Brookhaven National Laboratory. ERDA-1540, November 1975.

APPENDIX A

The following tables and figures present the data collected during the course of this study. Table A-1 tabulates the Ge(Li) gamma spectra taken at the two facilities. The annihilation gamma peak was the only one detected. Facility operation data are also listed in the table. Figure A-1 presents the gamma ray spectrum of the February 6th activated charcoal sample (#129).

Table A-2 presents the results of the tritium analyses, and Table A-3 presents the results of the ^{14}C analyses performed on selected molecular sieve (NaX) samples.

ID#	DATE	SAMPLE	SAMPLING TIME (hrs:min)	DECAY TIME (min)	COUNT TIME (secs)	PEAKS IDENTIFIED (other than background)	COMMENTS
				Cyclotron			
93	1/27	NaX-A	1:0	10	300		120 MeV alpha beam at
94	1/27	NaX-B	1:0	17	300		.02 uA (at cobalt target)
95	1/27	NaX-B	1:0	23	300		
96	1/27	HEPA	1:0	29	300		
97	1/27	Gas-1	n/a	1	300		
98	1/27	Gas-1	n/a	6	300		
99	1/27	Gas-2	n/a	0	600		
100	1/27	Gas-2	n/a	10	600		
101	1/27	Charcoal-A	2:59	6	600	.511 MeV	Trace peak - decayed with
102	1/27	Charcoal-A	2:59	16	400	.511 MeV	10-15 min half-life $^{13}N \sim$
103	1/27	Charcoal-B	2:59	25	600		10^{-9} µCi/cc $\pm$ 50%*
105	1/30	NaX-A	2:12	2	300		65 MeV proton beam at .02
106	1/30	NaX-A	2:12	7	300		uA (at spectrometer)
107	1/30	HEPA	2:12	12	300		
108	1/30	Charcoal-A	2:28	2.5	300	.511 MeV	Trace peak - decayed with
109	1/30	Charcoal-A	2:28	7.5	300	.511 MeV	5-10 min half-life $^{13}N \sim$
110	1/30	HEPA	2:28	14	300		10^{-9} µCi/cc $\pm$ 100%

Ge(Li) SPECTROMETRY DATA

ID#	DATE	SAMPLE	SAMPLING TIME (hrs:min)	DECAY TIME (min)	COUNT TIME (secs)	PEAKS IDENTIFIED (other than background)	COMMENTS
111	1/30	Background	n/a	n/a	10,000		
112	1/30	HEPA	2:12	63	10,000		
113	1/31	Charcoal-A	17:32	2	300	.511 MeV	Trace peak - decayed with 5-10 min half-life ^{13}N $\sim$
114	1/31	Charcoal-A	17:32	7	300	.511 MeV	10^{-9} uCi/cc $\pm$ 100%
115	1/31	NaX-A	17:49	3	300		
116	1/31	Gas	n/a	.5	600		
117	1/31	Background	n/a	n/a	n/a		
119	2/6	NaX-A	0:58	2	300	.511 MeV	100 MeV proton beam at 1.9 uA with Be/Al target produc-
120	2/6	NaX-A	0:58	7	300	.511 MeV	ing high energy neutrons,
121	2/6	NaX-A	0:58	13	300	.511 MeV	about 2×10^{12} n/sec at 100 MeV
122	2/6	NaX-A	0:58	19	300	.511 MeV	(see Figure 5-5)
123	2/6	Background	n/a	n/a	1,000		^{11}C conc.=5×10^{-8} μCi/cc**
124	2/6	Gas-1	n/a	1	300	.511 MeV	Decayed with 96 sec half-
125	2/6	Gas-1	n/a	6	300	.511 MeV	life - ^{15}O (see Figure 5-4)
126	2/6	Gas-2	n/a	0	300		Conc.=2×10^{-6} μCi/cc+
127	2/6	Gas-2	n/a	6	300		Beam off during sampling
128	2/6	Gas-2	n/a	12	300		
129	2/6	Charcoal-A	2:57	2	300	.511 MeV	Decayed with 10 min half-
130	2/6	Charcoal-A	2:57	7	300	.511 MeV	life - ^{13}N (see Figure 5-4)
131	2/6	Charcoal-A	2:57	12	300	.511 MeV	Conc.=3×10^{-8} μCi/cc
132	2/6	Charcoal-A	2:57	17	300	.511 MeV	

TABLE A-1 (Continued)

Ge(Li) SPECTROMETRY DATA

ID#	DATE	SAMPLE	SAMPLING TIME (hrs:min)	DECAY TIME (min)	COUNT TIME (secs)	PEAKS IDENTIFIED (other than background)	COMMENTS
133	2/6	Charcoal-B	2:57	22	300	.511 MeV	Assume ^{13}N
14	2/22	NaX-A	1:37	2	300		80 MeV alpha beam at .2 uA
16	2/22	NaX-A	1:37	7	300		
17	2/22	HEPA	1:37	13	300		
18	2/22	Charcoal-A	2:38	2	300		
19	2/22	HEPA	2:38	8	300		
			Van de Graaff				
	3/6	Charcoal-A (cavity exh.)	1:33	2	300		4.7 MeV proton beam at 1.7 uA with H-3 target producing 4 MeV neutrons
	3/6	Charcoal-A	1:33	7	300		
	3/6	HEPA	1:33	24	300		
	3/7	NaX-A (cavity exh.)	17:20	5	300		No beam - target downloading
	3/7	HEPA	17:20	10	300		
58	3/7	Charcoal-A (vacuum exh.)	3:57	2	300		
59	3/7	HEPA	3:57	15	1000		
60	3/7	Background	n/a	n/a	10,000		
61	3/13	Charcoal-A (vacuum exh.)	1:37	2	500		3 MeV deuteron beam at 3 uA with deuterium target producing 6 MeV neutrons beam off 3/13, 2400 hrs

ID#	DATE	SAMPLE	SAMPLING TIME (hrs:min)	DECAY TIME (min)	COUNT TIME (secs)	PEAKS IDENTIFIED (other than background)	COMMENTS
62	3/13	HEPA	1:37	12	500		
65	3/14	NaX-A (cavity exh.)	24:28	1	500		
66	3/14	HEPA	24:28	10	500		

Sample Calculations:

$$*C = \frac{140}{600} \text{ (cps)} \times 12.4 \text{ (decay correction)}/3.7\times10^4 \left(\frac{cps}{\mu Ci}\right) \times .0171 \text{ (det. eff.)} \times .83 \text{ (coll. eff.)} \times 5.2\times10^6 \text{ (cc)}$$

$$= 1.1 \times 10^{-9} \; \mu Ci/cc$$

$$\text{(decay corr.} = \quad \lambda t/1-e^{-\lambda t} = .00116(s^{-1}) \times 10,740(s)/1-10^{-6} = 12.4$$

$$**C = \frac{580}{300} \text{ (cps)} \times 2.3 \text{ (decay corr.)}/3.7\times10^4 \times .0171 \times .08 \times 1.64 \times 10^6 \text{ (cc)}$$

$$= 5.4 \times 10^{-8} \; \mu Ci/cc$$

$$+C = \frac{205}{300} \text{ (cps)}/3.7\times10^4 \times .0048 \text{ (det. eff.)} \times 2000 \text{ (cc)} = 1.9\times10^{-6} \; \mu Ci/cc$$
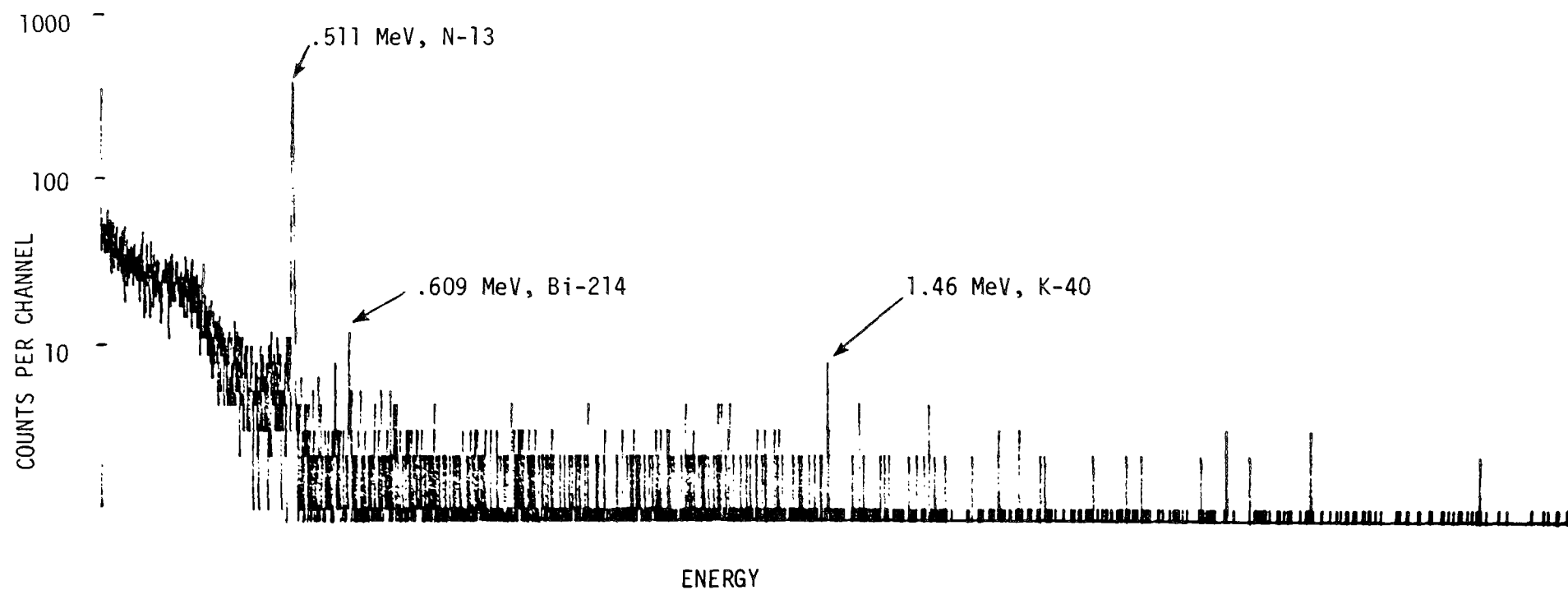
FIGURE A-1

4096 CHANNEL GAMMA SPECTRUM, #129, 300 sec.

TABLE A-2

RESULTS OF TRITIUM ANALYSES

Sample No.	Date	Location	Sampling Time (hrs:min)	Tritium Concentration $\mu Ci/cc$	Ventilation Flow cc/min
			Cyclotron		
3	1/27	Main Exhaust	3:00	$<7 \cdot 10^{-9}$	$4.8 \cdot 10^{8}$
10	1/30-31	Main Exhaust	20:00	$<1 \cdot 10^{-9}$	$4.8 \cdot 10^{8}$
14	2/6-7	Main Exhaust	16:25	$<1 \cdot 10^{-9}$	$4.8 \cdot 10^{8}$
20	2/22	Main Exhaust	2:37	$<8 \cdot 10^{-9}$	$4.8 \cdot 10^{8}$
			Van de Graaff		
3	3/6-7	Cavity Exhaust	16:04	$6 \cdot 10^{-8}$	$1.1 \cdot 10^{8(*)}$
5	3/7-8	Cavity Exhaust	26:37	$\geq 2 \cdot 10^{-8}(+)$	$1.1 \cdot 10^{8(*)}$
6	3/7-8	Hood Exhaust	26:12	$\geq 2 \cdot 10^{-5}(+)$	$1.7 \cdot 10^{7}$
7	3/7-8	Vacuum Pump Exhaust	23:19	$6 \cdot 10^{-7}$	~ 0
10	3/13-14	Cavity Exhaust	24:28	$1.5 \cdot 10^{-8}$	$1.1 \cdot 10^{8(*)}$
11	3/13-14	Cavity	26:15	$6 \cdot 10^{-8}$	$2.2 \cdot 10^{7}$

NOTE: [+]Saturation of silica gel with water vapor (HTO) occurred reducing collection efficiency to less than 100%.

*This represents the return air flow of a closed-cycle ventilation system.

TABLE A-3

RESULTS OF CARBON-14 ANALYSES

Facility	Date	Sample Time (hrs:min)	Volume CO_2 (cc)	C-14 Concentration pCi/ℓ CO_2	C-14 Concentration pCi/m^3 air
Cyclotron	1/30	2:12	1.0	<69	0+145
Cyclotron	2/6	16:13	22.5	<9	0+2
Van de Graaff	3/6	16:04	18.1	320+32	100+10
Van de Graaff	3/13	24:28	7.03	<57	0+12
Control Sample (Blank)	-	-	14.4	<14	0+4

APPENDIX B

Sampling Techniques

The absorber sampling was performed using three different types of media. These included sodium zeolite for trapping CO_2, charcoal for gases N_2 and O_2, and silica gel for tritiated H_2O.

The charcoal and the silica gel samplers were run in a sample train as shown in Figure 5-3. The charcoal sampler consisted of five media cups in a cylindrical body with two end caps. "O" rings served as seals between the cups and end caps, forcing all flow through the sample media. Sample media, in direction of flow, included a blank cup, particulate filter, primary charcoal, back-up charcoal, blank cup. The sampling rate for this canister was $\simeq 28$ L/m. After passing through the charcoal, a side stream flow was passed through a rotameter, followed by a tritium sample cartridge. The tritium sampler consisted of a 30 cm pipe nipple, two end caps with appropriate tube fittings, silica gel (Grade 05, 6-16 mesh), filters, snap rings, screens, and tell-tale desiccant (Grade 42, 6-16 mesh). The sampling rate through the tritium sampler was $\simeq 7$ L/m. The sampling probe consisted of a 9.5 mm aluminum tube bent in such a way as to facilitate isokinetic air sampling.

An identical type probe was used for sampling air through the sodium zeolite cartridge. The sampler was the same type as used in the charcoal sampler described above. Sample media, in direction of flow, included a blank cup, particulate filter, primary sodium zeolite (NaX), back-up NaX, blank cup. Air was drawn through this sampler at a rate of $\simeq 28$ L/m.

The duration of sampling was in the range of 1 to 2 hours. Because of the short-lived activities of O^{15}, N^{13}, and C^{11}, an attempt was made to begin the gamma analysis as soon as possible after sampling. The delay was normally less than 2 minutes.

One or a mixture of the three isotopes mentioned above was indicated by presence of the annihilation peak at 511 KeV. The sample was recounted sequentially for 5 minutes with each spectrum being stored on magnetic tape. This procedure was continued until the 511 KeV peak returned to background. Subsequent analyses of each spectrum was used to obtain a decay curve and thus to determine the composition of the isotopes in the air sampled.

The tritium samples were returned to the NES laboratory for processing. The dry silica gel had been weighed before being loaded into the sampler. The sampling duration and flow rate were recorded in a log. The outlet end of the samplers were opened and the snap ring, filter, and screen were removed to check the condition of the tell-tale indicator, which was noted in the sample log book. The dry, blue indicator turns through pink to white as it becomes saturated with H_2O. The contents of the sampler were then dumped into a wide mouth 4-liter bottle for mixing to obtain a homogeneous sample for analysis. A 3 gram ($\pm$ 0.1 g) sample of silica gel was weighed out into each of three liquid scintillation vials. Two milliliters ($\pm$ 0.1 ml) distilled water and ten milliliters ($\pm$ 0.1 ml) of scintillation cocktail solution were added to each. The vials were capped and shaken adsorbing the tritium from the silica gel into the scintillation cocktail. The samples were then allowed to stand for 4 hours to assure equilibrium between silica gel and cocktail solution. The samples were then counted on a liquid scintillation counter. An NBS tritium standard and a blank were also counted with the samples, the blank being taken as the background tritium activity.

The second type of sampling that was performed was the direct extraction of a gas sample into an evacuated glass marinelli container. This sampler has a cylinder in the middle which fits over the Ge(Li) gamma ray detector. This geometry optimizes the efficiency of analyzing a gas sample. To collect a gas sample the container was simply evacuated with a vacuum pump and the stopcock was then closed. The sampler was then connected to a probe in the air duct to be sampled and the stopcock opened drawing air into the container. The stopcock was again closed and the container quickly moved to the gamma-ray detector for counting.

Flow measurements in the air ducts sampled were made using a pitot tube. Air velocity was measured at several penetration depths and an average was taken. The velocity was multiplied by the cross-sectional area of the duct to obtain the flow rate.